AMERICAN UNIVERSITY OF BEIRUT

UNCERTAINTY QUANTIFICATION OF THE BOND STRESS – DISPLACEMENT RELATIONSHIP OF SHORING ANCHORS IN DIFFERENT GEOLOGIC UNITS

by
RIM WALID CHAHBAZ

A thesis
Submitted in partial fulfillment of the requirements
for the degree of Master of Engineering
to the Department of Civil and Environmental Engineering
of the Maroun Semaan Faculty of Engineering and Architecture
at the American University of Beirut

Beirut, Lebanon
April 2019

AMERICAN UNIVERSITY OF BEIRUT

UNCERTAINTY QUANTIFICATION OF THE BOND STRESS – DISPLACEMENT RELATIONSHIP OF SHORING ANCHORS IN DIFFERENT GEOLOGIC UNITS

by

RIM WALID CHAHBAZ

Approved by:

Dr. Shadi Najjar, Associate Professor — Advisor
Department of Civil and Environmental Engineering

Dr. Salah Sadek, Professor — Advisor
Department of Civil and Environmental Engineering

Dr. Ibrahim Alameddine, Professor — Member of Committee
Assistant Professor of Civil & Environmental Engineering

Date of thesis defense: April 25th, 2019

AMERICAN UNIVERSITY OF BEIRUT

THESIS, DISSERTATION, PROJECT RELEASE FORM

Student Name: Chahbaz (Last) Rim (First) Walid (Middle)

● Master's Thesis ○ Master's Project ○ Doctoral Dissertation

☑ I authorize the American University of Beirut to: (a) reproduce hard or electronic copies of my thesis, dissertation, or project; (b) include such copies in the archives and digital repositories of the University; and (c) make freely available such copies to third parties for research or educational purposes.

☐ I authorize the American University of Beirut, to: (a) reproduce hard or electronic copies of it; (b) include such copies in the archives and digital repositories of the University; and (c) make freely available such copies to third parties for research or educational purposes
after:

One ---- year from the date of submission of my thesis, dissertation, or project.
Two ---- years from the date of submission of my thesis, dissertation, or project.
Three ---- years from the date of submission of my thesis, dissertation, or project.

Rim Chahbaz 5/21/2019

Signature Date

ACKNOWLEDGMENTS

First, I would like to express my deep appreciation and gratitude to my professors, Dr. Shadi Najjar and Dr. Salah Sadek for their guidance and assistance during the whole thesis phases. Also, for making me always proud to be one of their students.

Second, my very profound gratitude to my parents, to my fiancé and my family for their continuous support and continuous encouragement throughout my years of study and through the process of researching and writing this thesis. Nothing would be possible without them. Thank you

AN ABSTRACT OF THE THESIS OF

Rim Walid Chahbaz for Master of Engineering
Major: Geotechnical Engineering

Title: Uncertainty Quantification of the Bond Stress – Displacement Relationship of Shoring Anchors in Different Geologic Units

The design of anchored wall systems in shoring applications is generally governed by the bond strength between the grout and the surrounding soil/rock in the grouted bond zone. Published work on the reliability of anchored retaining systems focuses on ultimate limit state considerations to ensure a target level of safety/reliability against pullout of the anchor in the bonded zone at the grout/soil interface. These studies do not shed light on the variability of the bond strength at different levels of anchor slip (deformation) at the grout/soil interface. The primary objective of this paper is to quantify the uncertainty in the bond strength that is mobilized at target values of anchor slip to aid the serviceability limit state design of anchored wall systems. To achieve this objective, a database of actual shoring anchor tests from real projects that were executed in several sites around Beirut is assembled and analyzed to quantify the uncertainty in the mobilized bond strength at target levels of anchor deformation. The tests are categorized based on three different geologic units (Limestone, Marls, and Clays) that are common to many geologic settings in the world. The bond stress – displacement relationship is modeled with a hyperbolic model and the statistics of the model are derived from the assembled database and classified based on the geologic units analyzed. The secondary objective of this research is to show the effect of this uncertainty on a real anchored retaining wall example to reflect it on the reliability-based design of this example.

CONTENTS

Illustrations

Figure

Tables

Table

CHAPTER 1
INTRODUCTION

1.1 Background

Lateral shoring systems which incorporate ground anchors provide practical solutions for controlling lateral deformations in open excavations and stabilizing slopes and retaining systems (Sabatini et al. 1999, Tang and Phoon 2016, and Liu et al. 2017). Ground anchors play a central/critical role in the overall stability and deformation control of the shoring system. Despite this critical role, the methodologies that are currently used for analyzing and designing ground anchors are limited to ultimate limit state criteria which specify the ultimate load capacity of the anchor based on an assumed ultimate bond stress between the anchor and the surrounding rocks or soils. Once an ultimate bond stress is selected, the length of the anchor in the bonded zone is selected based on an assumed factor of safety against ultimate pullout of the anchor. Liu et al. (2017) states that the main limitation of this approach lies in the selection of the ultimate bond stress which generally spreads in a relatively wide range.

In order to address/minimize the impact of design uncertainties, field tests of anchors are mandated as part of the execution methodologies and specifications. These tests typically include pullout tests (failure tests) and proof tests (stressing to >125% of service design capacity). Several published studies have studied the sources of uncertainty that are associated with the design and performance of ground anchors. Examples include the work of Briaud, Powers, and Weatherby (1998), Kim (2003), Liu, Xiaoming, et al. (2017), Cherubini, Garrasi, and Petrolla (1992), Kwon, Minho, et al. (2017), Munwar Basha and Sivakumar Babu (2008), Hegazy (2003), Basma (1991), and Ching, Hung-Jiun, and Chia (2008).

The uncertainties in the design of ground anchors may be addressed by improving the current understanding of the load transfer between ground anchors and rocks/soils at different levels of anchor displacement in the bonded zone. With the advancement of performance based design in geotechnical engineering, better understanding of the mobilization of bond stress with anchor displacement in the bonded zone is needed to allow for checking serviceability-based design considerations for retaining systems that are supported with ground anchors. A review of the literature indicates that there is lack of studies that target the bond stress-bond displacement relationship for ground anchors in different geologic units. There are very limited experimental data from full scale tests on the performance and behavior of ground anchors, particularly in geologic settings that involve rocks (Liu et al. 2017) and other sedimentary units that involve stiff marls and clays.

The primary objective of this paper is to quantify the uncertainty in the bond stress –displacement relationship of ground anchors to aid the serviceability limit state design of anchored wall systems. To achieve this objective, a database of actual shoring anchor tests from real projects that were executed in several sites around Beirut is assembled and analyzed. The tests are categorized based on three geologic units (Limestone, Marls, and Clays) that are common to many geologic settings in the world. The bond stress – displacement relationship is modeled with a hyperbolic model and the statistics of the model are derived from the assembled database and classified based on the geologic units analyzed. The proposed work is intended to help move the field towards a greater understanding and appreciation of the importance of variability in anchor design and suggested means to incorporate it in actual practice.

1.2 Objectives of this thesis

This proposed research mainly aims to characterize the uncertainty in the bond strength of anchors in three different geologic settings. These geologic settings/strata are: Limestone, Marl, and Clay. This characterization of uncertainty will be done relying on the results from actual pullout tests that were assembled in a database which was collected from a number of shoring contractors in Lebanon.

The second objective of this research is to incorporate the uncertainty in the displacement in the bonded zone to reflect it in the reliability-based design of an anchored retaining wall.

1.3 Proposed scope of work

Step 1: Conduct a literature review targeting the reliability-based design of anchors design and its workability. This step is done basically in order to understand all the different methodologies that are proposed in the literature review.

Step 2: Collecting data from actual sites in Lebanon. To achieve the goal of this study, it is required to collect data in a form of test reports and geotechnical reports from actual sites in Lebanon. The soil of these sites should belong to three soil types: Limestone, Marl, and Clay. Collecting data will reduce significantly the uncertainty. This step will be achieved depending on the data available at engineering companies that perform pullout tests.

Step 3: Compiling test data in data base. The obtained data will be arranged in Excel as a database. All the available information of each test, including the type of soil, the location, the date of the test, the level of the test, the ultimate load, the displacement variation, and the graphs…, will be compiled to be used later for the probabilistic analysis.

Step 4: Dividing them into categories. The tests will be divided into three categories depending on the soil type where the pullout tests were performed. This will be done by counting on the information mentioned in the test report, in the available geotechnical reports and depending on the obtained ultimate strength.

Step 5: Analyzing the results statistically to quantify the uncertainty in the observed stress-displacement curves. The analysis will be done after plotting for each type of soil the stress-displacement curves for all the tests and normalizing these curves using a hyperbolic model. The uncertainty in the stress-displacement curves is illustrated by the uncertainty in the hyperbolic parameters.

Step 6: Applying the obtained results on a real example. The obtained statistical model will be used to study the stability of a real anchored wall. Also, this example is to show the importance of probabilistic approach in the design by checking the probability of failure of the wall.

1.4 Significance of the Proposed Research

Previously published studies focused on investigating the variability of soil parameters (angle of friction, unit weight…), design parameters (bond length, drilling diameter…) and the presence or absence of water table. But these models in the literature did not clarify the variability of the bond strength at different levels of anchor slip (deformation) at the grout/soil interface. Anyhow, the proposed work will add a new angle of looking at the performance of anchors during the pullout test. Also, it will shed the light the bond strength of anchors on a certain displacement. And this will be done for each geologic unit.

CHAPTER 2
LITERATURE REVIEW

3.1 Introduction

This section aims to compile and show all the previous work done that focus on the workability and the uncertainty of the anchors in addition to the reliability-based design of anchors. Basically, this work will help to highlight the key findings and the development of the proposed topic. Also, it will indicate all the limitations concerning the studies done on anchors.

3.2 Performance of Anchors under Certain Conditions

Briaud, Powers, and Weatherby (1998) presented a set of tests on ten short and long bonded length anchors performed in clay at the National Geotechnical Experimentation Site at Texas A&M University. In this study, α values (the ratio of grout interface f_{max} over shear strength Su) for low-pressure and straight-shaft grouted anchors were compared with data from drilled shafts by Kulhawy and Jackson (1989) and by Reese and O'Neill (1988) (See Figure 1). Also, they focused on the creep movement due to sustained tensile loads on the anchors and the variations of creep movement as a function of time (see Figure 2). The load distribution in the grout and in the steel tendon was considered and plotted (See Figure 3). Moreover, a comparative study between the short and long bonded length anchors was made to show the influence of bond length on the obtained ultimate load, creep rate, and lower-time dependent load loss. It also showed the influence of reloading on creep movement (See Table 1). In conclusion, the stresses in the soil were concentrated near the barrier between the bonded length and the unbonded length. In addition, for short bonded

anchors, the ultimate soil resistance was 23% larger than the one for long bonded length. For the same overall length, the grouted anchors with a short tendon bond length had the higher ultimate load, lower creep rate, and lower time-dependent load loss. Also, it was concluded that the anchor should be short enough to ensure the required safety.

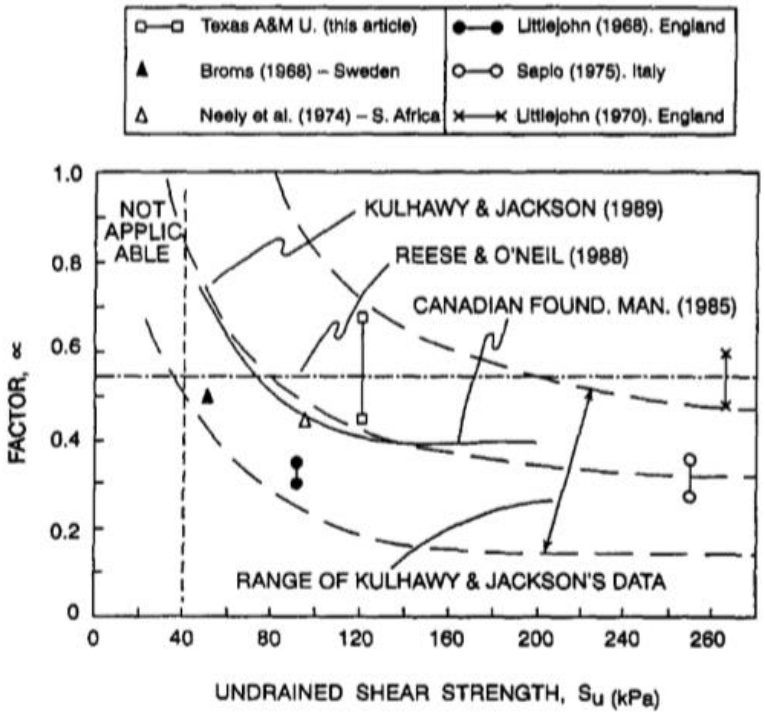

Figure 1 α Values for Low Pressure Grouted Anchors in Clay

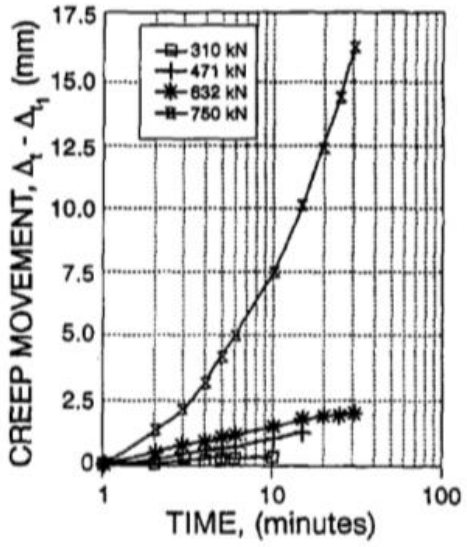

Figure 2 Creep Movement versus Time Curves for Anchor 5

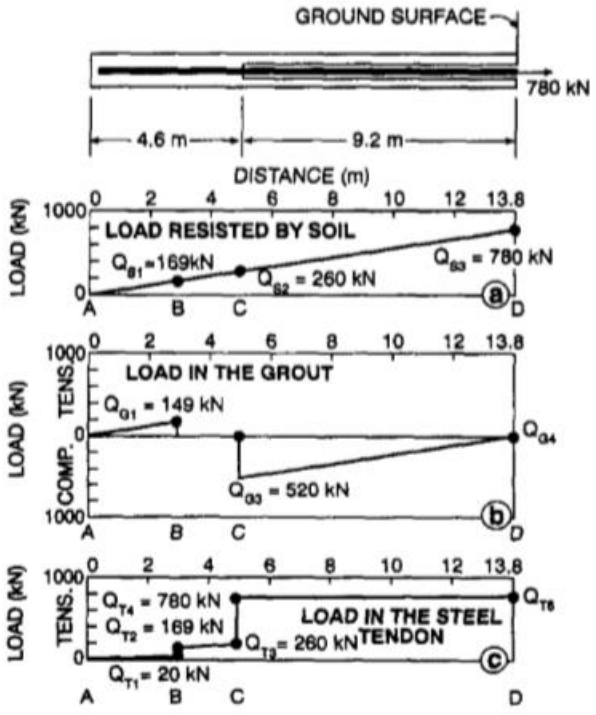

Figure 3 Load distribution near the ultimate load

Table 1 Data for 10 Anchors

Anchor number (1)	Ultimate load (kN) (2)	Bonded anchor length (m) (3)	Friction stress at failure (kN/m²) (4)	α values (5)
1	867	4.57	65.9	0.53
2	1080	4.57	82.1	0.66
3	ID[a]	4.57	—	—
4	934	4.57	71.0	0.57
5	ID[a]	4.57	—	—
6	712[b]	4.57	54.1	0.43
7	801	9.15	60.9	0.49
8	747	9.15	56.8	0.45
9	ID	9.15	—	—
10	801	9.15	60.9	0.49

[a]Insufficient displacement
[b]Installation difficulties encountered; 60% of anchor not grouted under pressure but simply free-fall.

Kim (2003) displayed a set of tests on tension anchors and compression anchors (performance tests, creep tests and long-term relaxation tests) (See Table 2). He explained, in his research, the current design practice. Moreover, Pullout tests were performed and the results are represented in Figure 4 and Table 3. The obtained results from the load tests are used to identify the load distribution and consequently the load transfer mechanism (See Figure 5). A comparison was made between the load distributions of these two types of anchors. He also compared their creep rate and load loss. And to verify the load transfer obtained from test the beam-spring numerical model was used. Based on the results, the creep rate of compression anchors is observed to be smaller than the creep rate of tension anchors. In addition, the maximum friction resistance and the effective overburden pressure in the weathered soil are proportional.

Table 2 Types of test anchors

Anchor number	Type of anchor	Length (m)	Unbonded length (m)	Bonded length (m)	Number of strand
1	Tension	12	8	4	5
2	Compression	12	—	—	5
3	Compression	12	—	—	4
4	Compression	12	—	—	4
5	U-Turn Type	11.5	—	—	4
6	Tension	12	9	3	7
7	Tension	9	6	3	7

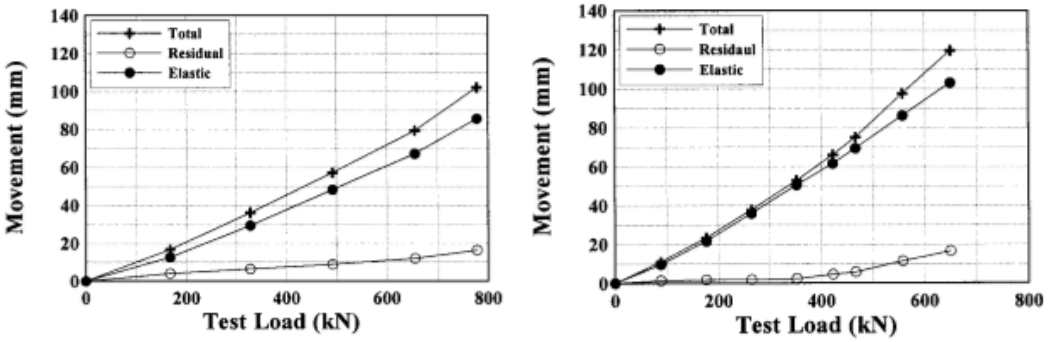

(a) Anchor No.1

(b) Anchor No.3

Figure 4 Components of anchor movement

Table 3 Ultimate loads from load test data

Anchor number	Q_{ult} (kN)	L_a (m)	$N_{(avg)}$ value	σ'_{ov} (kN/m^2)	f_{max} (kN/m^2)	$K=f_{max}/\sigma'_{ov}$	L_{bt} (m)
1	780	4	35	220	376	1.7	—
2	630	—	33	217	—	—	3.3
3	628	—	33	217	—	—	3.3
4	625	—	33	217	—	—	3.3
5	436	—	33	217	—	—	—
6	590	3	32	220	380	1.72	—
7	370	3	24	142	238	1.68	

Note: σ'_{ov} was calculated at the middle of bonded length. Bonded transmission length was calculated by using K-value of 1.7. L_a is a bonded length of tension anchor. L_{bt} is a bonded transmission length of compression anchor.

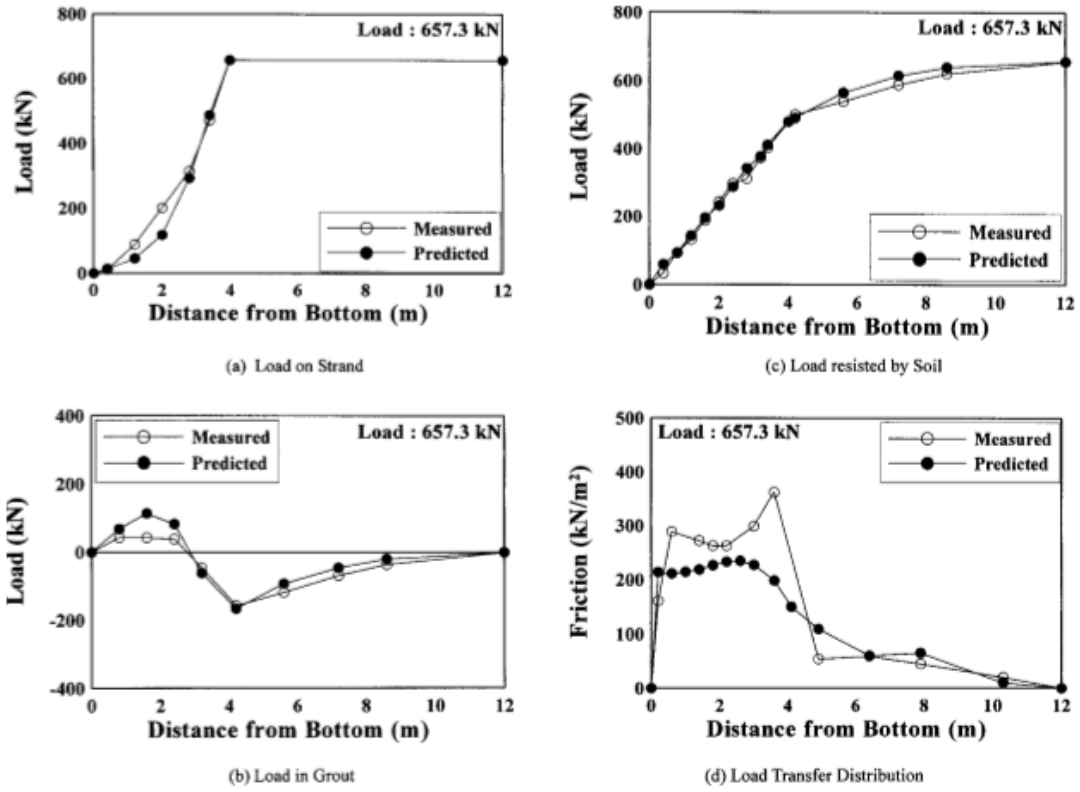

Figure 5 Variation of load as a function of distance from bottom

Liu, Xiaoming, et al. (2017) performed pullout tests on 3 anchors with the same bonded length in weathered limestone to compare their behavior under ultimate conditions. The test results presented an unexpected behavior of one of the three anchors and this behavior is due to the quality of the grouting (see Figure 6). Moreover, to identify the elastic-plastic zones an analytical model was developed and the derived solutions were validated using FLAC3D. Based on this analysis, it was concluded that the plastic zone depends on the bonded length and the diameter of the anchor but the elastic zone was independent of the bonded length. Furthermore, the ultimate bond strength was influenced by the anchor diameter and its bonded length (see Figure 7).

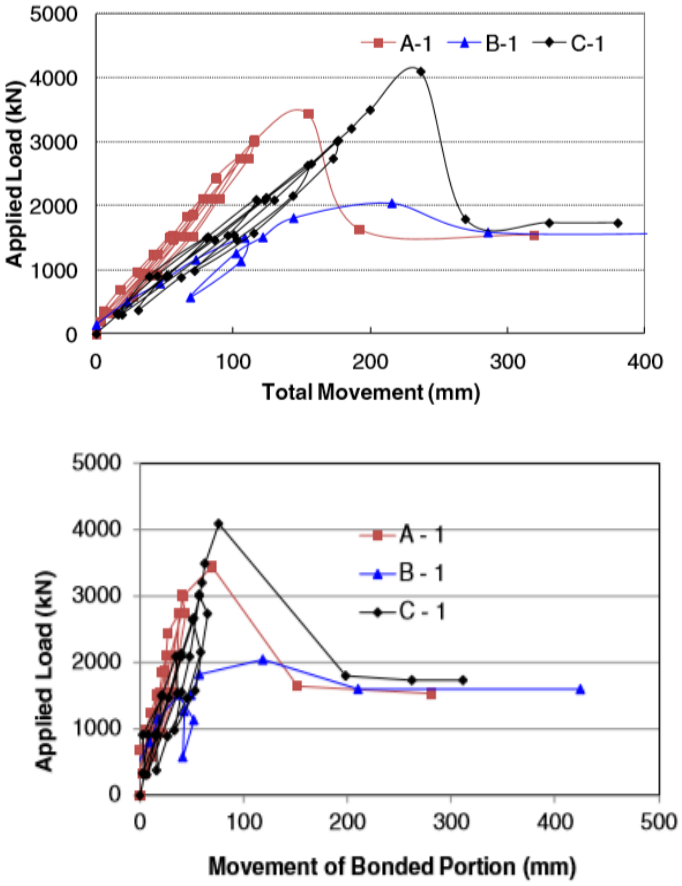

Figure 6 Load vs. displacement curve for three tested anchors: (a) load vs. total movement; and (b) load vs. movement of bonded portion.

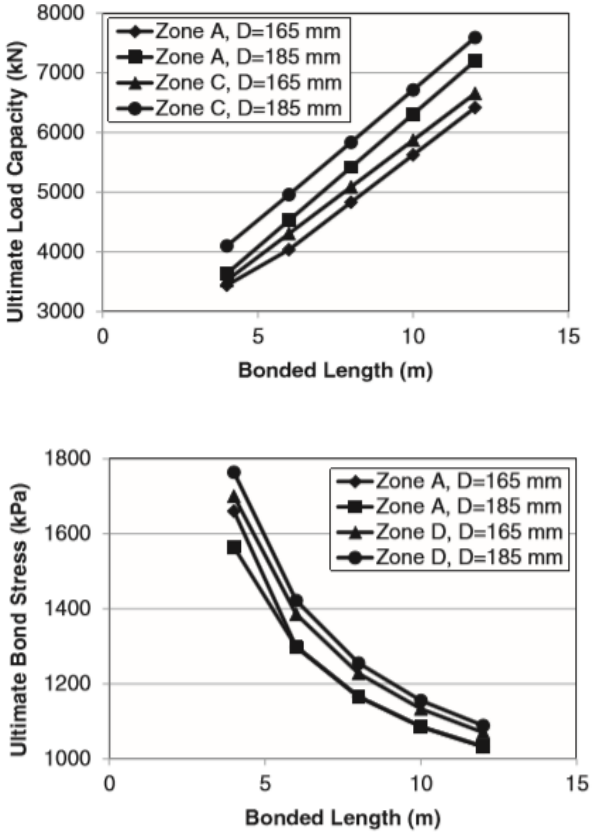

Figure 7 (a) bonded length vs. ultimate load capacity (b) bonded length vs average ultimate bond stress

Zhao, Wen, et al. (2017) showed the influence of anchorage failure on the stability of a deep excavation in sandy soils retained by anchored pile walls and the mechanical behavior of the retaining structure. A finite element method using PLAXIS was used to identify the mechanical behavior due to the anchorage failure types. Then, a comparison was done between the effect of individual anchor failure and anchor group failure on the deformations and bending moment and the mechanical responses in the supporting structure (see Figure 8). Based on the analysis, the deformation and bending moment in case of the group anchorage failure was larger than the ones in case of individual anchorage failure. On the other hand, they had the same mechanical response. Also, the factors of safety of all the anchorage failure cases were calculated and they ranged from 1.17 to 1.54. According to these factors of safety, it was

concluded that the anchorage failure affected the stability of the excavation; in the case of individual anchor failure, the stability was larger.

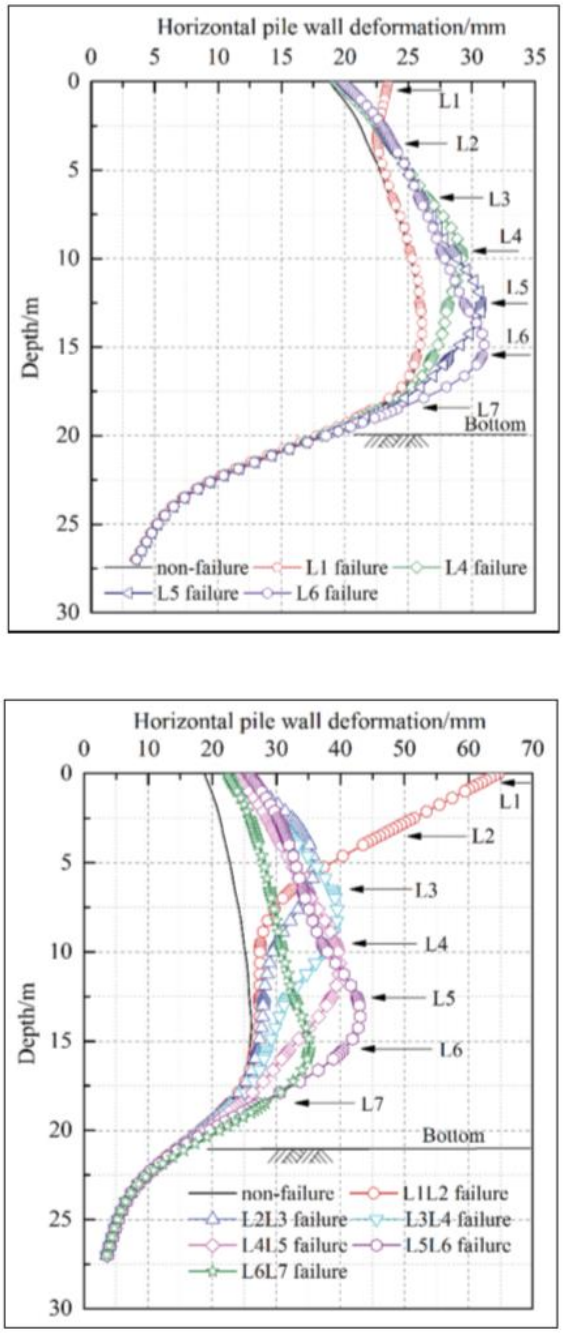

Figure 8 (a) Horizontal pile wall deformation of one-raw anchorage failure (b) Horizontal pile wall deformation of two-raw anchorage failure

Kwon, Minho, et al. (2017) performed a comparative pullout test on two types of specimens. One of them was executed considering the freeze and thaw effect to

study the long-term behavior of anchors. Pullout tests were performed to compare the behavior of these two types of the specimen. It was shown that due to the construction errors the performance of anchors was not always the same even if the diameter and length of insertion of the anchor were the same. Also, results showed decreased values of pullout strength and compressive strength compared to the values obtained from original specimens (around 50%) due to the effect of freeze and thaw on the concrete (See Figure 9 and 10). Moreover, a probabilistic approach was investigated. The standard deviation and coefficient of variation of pullout strength for specimens were calculated (See Table 4). This probabilistic approach leads to the ability to propose new capacity computation equations.

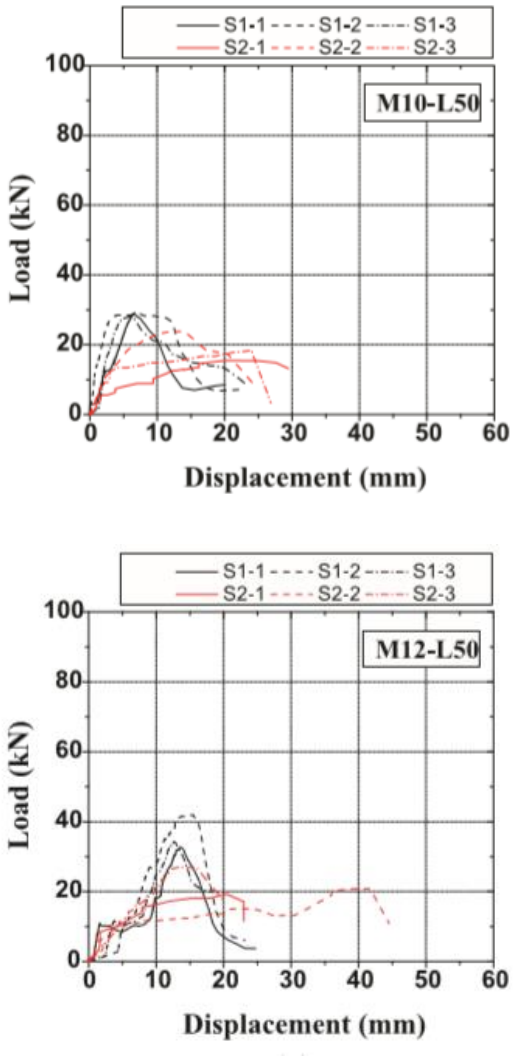

Figure 9 Load–displacement relation of the experimental results (a) Original (b) Freeze and thaw

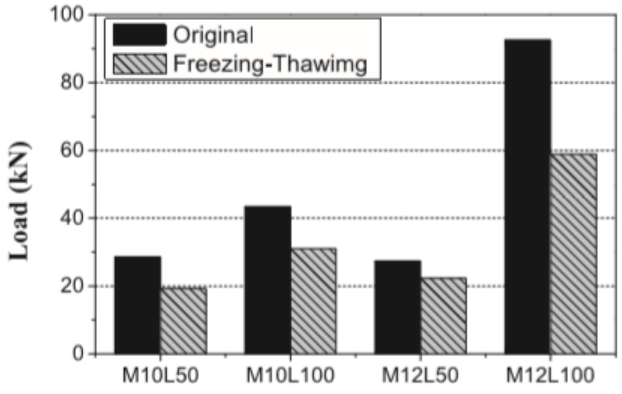

Figure 10 Comparison of the experimental results

Table 4 Comparison results of mean value, standard deviation, and coefficient of variation of the pullout strength

Type of specimen	Specimen	Mean value (kN)	Standard deviation (kN)	Coefficient of variation
Original	S1M10L50	28.6	0.58	0.020
	S1M10L100	43.4	5.35	0.123
	S1M12L50	37.3	4.71	0.126
	S1M12L100	92.6	0.64	0.007
Freeze–thaw	S2M10L50	19.2	4.22	0.219
	S2M10L100	31.0	1.87	0.060
	S2M12L50	22.3	4.07	0.183
	S2M12L100	58.9	9.70	0.165

3.3 Reliability-Based Design

Cherubini, Garrasi, and Petrolla (1992) investigated the stability of an anchored sheet-pile wall embedded in cohesionless soil based on the free earth support method. This investigation was done considering the variability of the soil physical and mechanical properties. Also, they illustrated the problems influencing the reliability of the anchor rod. The case study was used to compare the deterministic design with the reliability-based design. The reliability-based design was done considering the variability of the unit weight of the soil, the friction angle and the presence of water table (See Table 5 and Figure 11). Based on the analysis, it was shown that the resistive elements of the case were not strongly affected by the uncertainty of the soil unit weight and the presence or absence of the water table. In contrast, the soil-wall friction and the mean friction angle affected remarkably the probabilities of failure of the proposed structure (See Table 6).

Table 5 Coefficients of variation of some geotechnical parameters (modified from Vannucchi 1985)

Geotechnical property	Range of CV, %
Liquid limit	2–48
Plastic limit	8–29
Total unit weight	1–10
Natural water content	6–63
Void index	10–42
Grain size distribution	19–37
Friction angle (sand)	3–15
Effective cohesion (clay)	20–65
Effective friction angle (clay)	5–20

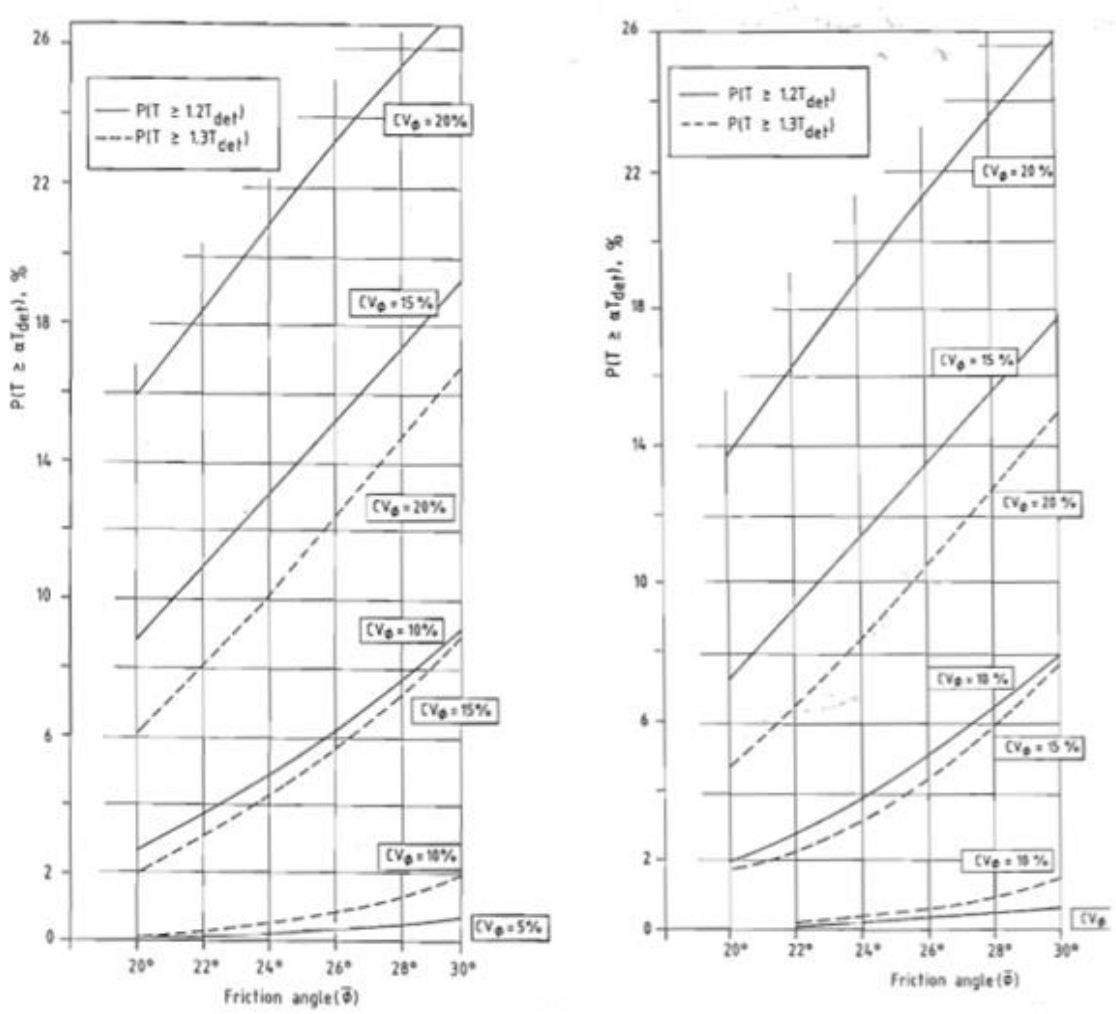

Figure 11 (a) Probability that the axial anchor load will reach certain levels in the first computation model CVγ = 5%; δ = φ; no ground water (b) Probability that the axial anchor load will reach certain levels in the first computation model CVγ = 5%; δ = φ; no ground water

Table 6 Values of reliability index for the first computational model for different δ and different CVφ

TABLE 2. Values of the reliability index for the first computational model, with $\delta = \phi$ and $CV_\gamma = 0$

$\bar{\phi}$	Water[a]	CV_ϕ, % 5	10	15	20
20	No	4.7906	2.4733	1.7337	1.3865
	Yes	4.7906	2.4734	1.7337	1.3866
22	No	4.1813	2.1777	1.5468	1.2573
	Yes	4.1812	2.1777	1.5468	1.2578
24	No	3.7394	1.9620	1.4092	1.1610
	Yes	3.7401	1.9624	1.4094	1.1612
26	No	3.4054	1.7996	1.3065	1.0903
	Yes	3.4058	1.7998	1.3066	1.0904
28	No	3.1279	1.6673	1.2257	1.0379
	Yes	3.1276	1.6672	1.2256	1.0378
30	No	2.8721	1.5495	1.1582	0.9984
	Yes	2.8705	1.5487	1.1577	0.9980

[a]Ground water present (yes) or absent (no).

TABLE 3. Values of the reliability index for the first computational model, with $\delta = 0.5\phi$ and $CV_\gamma = 0$

$\bar{\phi}$	Water[a]	CV_ϕ, % 5	10	15	20
20	No	5.2834	2.7150	1.8895	1.4977
	Yes	5.2837	2.7151	1.8896	1.4978
22	No	4.6057	2.3842	1.6783	1.3495
	Yes	4.6061	2.3844	1.6784	1.3495
24	No	4.1254	2.1475	1.5248	1.2397
	Yes	4.1258	2.1478	1.5250	1.2398
26	No	3.7697	1.9721	1.4111	1.1586
	Yes	3.7698	1.9721	1.4112	1.1587
28	No	3.4772	1.8300	1.3215	1.0974
	Yes	3.4778	1.8302	1.3217	1.0975
30	No	3.2076	1.7031	1.2458	1.0498
	Yes	3.2073	1.7030	1.2457	1.0498

[a]Ground water present (yes) or absent (no).

TABLE 4. Values of the reliability index for the first computational model, with $\delta = \phi$ and $CV_\gamma = 5\%$

$\bar{\phi}$	Water[a]	CV_ϕ, % 5	10	15	20
20	No	4.5395	2.4391	1.7229	1.3815
	Yes	4.5396	2.4391	1.7229	1.3815
22	No	3.9868	2.5111	1.5382	1.2532
	Yes	3.9867	2.1511	1.5382	1.2531
24	No	3.5829	1.9406	1.4022	1.1576
	Yes	3.5836	1.9409	1.4024	1.1577
26	No	3.2761	1.7819	1.3006	1.0873
	Yes	3.2766	1.7821	1.3007	1.0874
28	No	3.0209	1.6526	1.2207	1.0352
	Yes	3.0206	1.6525	1.2206	1.0352
30	No	2.7851	1.5375	1.1540	0.9960
	Yes	2.7835	1.5367	1.1535	0.9956

[a]Ground water present (yes) or absent (no).

TABLE 5. Values of the reliability index for the first computational model, with $\delta = 0.5\phi$ and $CV_\gamma = 5\%$

$\bar{\phi}$	Water[a]	CV_ϕ, % 5	10	15	20
20	No	5.0014	2.6766	1.8775	1.4922
	Yes	5.0017	2.6767	1.8776	1.4923
22	No	4.3814	2.3536	1.6685	1.3449
	Yes	4.3817	2.3538	1.6686	1.3450
24	No	3.9395	2.1222	1.5167	1.2358
	Yes	3.9399	1.1224	1.5168	1.2359
26	No	3.6114	1.9505	1.4041	1.1552
	Yes	3.6115	1.9506	1.4042	1.1553
28	No	3.3420	1.3154	1.0943	1.1432
	Yes	3.3425	1.8118	1.3156	1.0945
30	No	3.0944	1.6877	1.2406	1.0471
	Yes	3.0942	1.6875	1.2405	1.0470

[a]Ground water present (yes) or absent (no).

Munwar Basha and Sivakumar Babu (2008) discussed the need of reliability based design to study the stability of an anchored cantilever sheet pile wall in sandy soils. He focused on showing the influence of uncertainty in estimated soil parameters. Also, they focused on obtaining the optimal design parameters by working on a reliability-based optimized design. First, the reliability index should be calculated using the first order method. Then, the probability of failure should be calculated for each type of failure (See Table 8). Later, the target reliability index will be calculated (See Figure 12). This method of design is applied to a case study where all the

parameters are presented in Table 7. Consequently, the important role of the anchor was observed in all failure modes of sheet pile walls and in calculating the penetration depth and section modulus. On the other hand, the soil – steel pile interface friction angle seemed to significantly influence the rotational stability and the sliding stability of the sheet pile wall. In the same way, the fluctuation of the water table affects all of the failure modes.

Table 7 Statics of random input parameters

	Statistics		
Random variable	Mean, μ^a	Coefficient of variation, COV (%)	Distribution
γ	18 kN/m^3	7	Gaussian
γ_{sat}	19 kN/m^3	7	Gaussian
ϕ	30°	5 and 10	Log-normal
α	0 to 1 m	0.5	Gaussian
l_t	0.2H	0.5	Gaussian
f_y	415 kN/m^2	5	Gaussian
χ	—	0.5	Gaussian
T	—	5	Gaussian
S	—	5	Gaussian

Note: γ, unit weight of backfill soil; γ_{sat}, saturated unit weight; ϕ, friction angle of the soil; α, depth ratio of watertable from top of wall; l_t, depth of anchor from the top wall; f_y, yield strength of steel pile; χ, penetration depth ratio; T, anchor pull; S, section modulus of steel pile.

[a]Mean values of χ, T, and S should be obtained from TRBDO for the target component and system reliability indices (β_{rt}, β_{sli}, β_{fs}, and β_{sys}).

Table 8 Variation of reliability index with random variables considered in the optimization for rotational, sliding and flexural failure modes

Sensitivity of reliability index	Rotational failure mode	Sliding failure mode	Flexural failure mode
$\frac{\partial\beta}{\partial\gamma}$	–0.74	–1.40	–1.27
$\frac{\partial\beta}{\partial\gamma_{sat}}$	4.03	4.67	2.67
$\frac{\partial\beta}{\partial\phi}$	1.60	2.55	1.94
$\frac{\partial\beta}{\partial\alpha}$	–11.88	–28.44	–95.33
$\frac{\partial\beta}{\partial\chi}$	24.06	36.91	0
$\frac{\partial\beta}{\partial T}$	0	3.87	–24.70
$\frac{\partial\beta}{\partial l_t}$	11.84	0	0
$\frac{\partial\beta}{\partial f_y}$	0	0	0.18
$\frac{\partial\beta}{\partial S}$	0	0	48.25

Note: β, reliability index; γ, unit weight of backfill soil; γ_{sat}, saturated unit weight; ϕ, friction angle of the backfill; α, depth ration of watertable from top of wall; χ, penetration depth ratio; T, anchor pull; l_t, depth of anchor from top of wall; f_y, yield strength of steel pile; S, section modulus of steel pile.

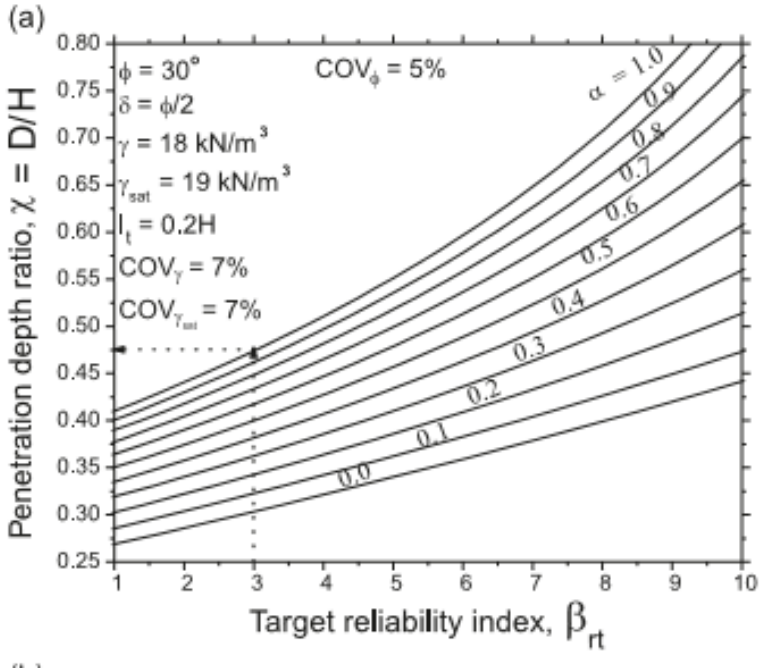

Figure 12 Total penetration depth ratio versus target reliability index against rotational failure

Prästings, Anders, Stefan Larsson, and Rasmus Müller (2016) presented the design of an anchored sheet pile wall in clay considering the uncertainty in undrained shear strength. After the observed variability in the obtained results of site investigations of the proposed project, additional investigations were needed to get the undrained shear strength. A multivariate analysis was proposed to show the reduced uncertainty due to the multivariate investigation (see Table 9 and Figure 13). Moreover, a reliability-based design method was completed using the first order second-moment approach to show the effect of combining the reliability-based design and the multivariate analysis in reducing the uncertainty and in saving in the design like reducing the penetration depth.

Table 9 (a) Uncertainty factors for the evaluation of COVSu in previous investigations (archive, 2011, and 2012). (b) Uncertainty factors for the evaluation of COVSu in additional investigations (archive, 2011, 2012, and 2014).

Uncertainty factors for the evaluation of $COV_{S_u|D_i}$ in previous investigations (*archive, 2011, and 2012*).

D_i	$\hat{\sigma}_i^2$ [a]	COV_{Di} [b]	n_i	$COV_{sp\|D_i}$	Γ_{v,D_i} [c]	$COV_{e,i}$ [d]	$COV_{tm,i}$ [e]
CPT	0.0159	0.127	64	0.048	0.41	0.05	0.10
FC	0.0391	0.200	25	0.077	0.41	0.07	0.16
FV	0.0180	0.134	16	0.036	0.41	0.10	0.17
P	0.0200	0.142	12	0.051	0.41	0.07	0.10

[a] According to Eq. (6).
[b] Evaluated from measurements (transformed to normality) according to Eq. (8) (Müller et al., 2014).
[c] Evaluated based on $\theta_{v,CPT}$ $\left(\Gamma_{v,D_i} = \sqrt{\theta_{v,CPT}/6} = \sqrt{1/6}\right)$.
[d] Phoon and Kulhawy (1999), values from *P* and *FC* are assumed similar to index tests.
[e] Larsson et al. (2007).

Uncertainty factors for the evaluation of $COV_{S_u|D_i}$ in additional investigations (*archive, 2011, 2012, and 2014*).

D_i	$\hat{\sigma}_i^2$ [a]	COV_{Di} [b]	n_i	$COV_{sp\|D_i}$	Γ_{v,D_i} [c]	$COV_{e,i}$ [d]	$COV_{tm,i}$ [e]
CPT	0.014	0.118	105	0.044	0.41	0.05	0.10
FC	0.034	0.188	38	0.071	0.41	0.07	0.16
FV	0.018	0.134	16	0.036	0.41	0.10	0.17
P	0.013	0.116	22	0.038	0.41	0.07	0.10
DSS	0.016	0.125	10	0.042	0.41	0.07	0

[a] According to Eq. (6).
[b] Evaluated from measurements (transformed to normality) according to Eq. (8) (Müller et al., 2014).
[c] Evaluated based on $\theta_{v,CPT}$ $\left(\Gamma_{v,D_i} = \sqrt{\theta_{v,CPT}/6} = \sqrt{1/6}\right)$.
[d] Phoon and Kulhawy (1999), values from *P* and *FC* are assumed similar to index tests.
[e] Larsson et al. (2007).

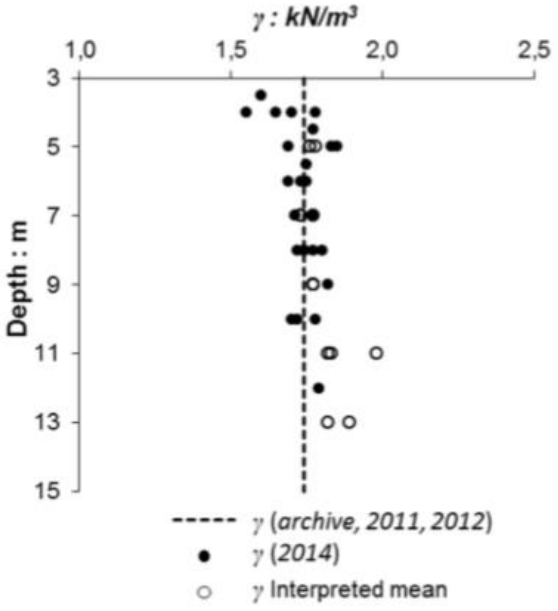

Figure 13 Measured index parameters in ‘‘Clay” from previous investigations (archive, 2011, and 2012) and additional investigations (2014): γ.

Hegazy (2003) collected in his study in-situ pullout test data for anchors in cohesive soil, cohesionless soil, and rock. The measured pullout resistance values of anchors were compared to the predicted values. The prediction of the values was done relying on the Post-Tensioning Institute (PTI) values of bond strength. A comparison between the measured pullout resistance and the presumptive resistance obtained from PTI was done. Figure 14 represents the three histograms showing the bias factor λ of anchor pullout resistance in Clay, Sands, and Rocks. Also, Table 10 summarizes the number of data for each type of soil, the mean and the coefficient of variation of the bias factor and the probability of failure PF. Considering that the resistance and the load are lognormally distributed, a probabilistic analysis was effected to determine the reliability indices β, the resistance factor φ and the factor of safety (see Table 11). Based on the analysis, the minimum recommended factor of safety for each type of soil and rock is increased in case of using the maximum presumptive bond strength while it is conservative in case of using the minimum and average presumptive values for clay and sand and minimum values for rock.

Table 10 Statistical properties of data bias

Material	Bias (λ)	No. of Data	μ (λ)	COV (λ)	PF
Clay	P_m / P_p-min	59	2.56	0.71	0.05
	P_m / P_p-avg	59	1.48	0.75	0.42
	P_m / P_p-max	59	1.05	0.75	0.66
Sand	P_m / P_p-min	84	2.2	0.74	0.08
	P_m / P_p-avg	84	0.94	0.49	0.67
	P_m / P_p-max	84	0.63	0.47	0.88
Rock	P_m / P_p-min	107	3.13	0.81	0.19
	P_m / P_p-avg	107	1.70	0.97	0.44
	P_m / P_p-max	107	1.21	1.02	0.63

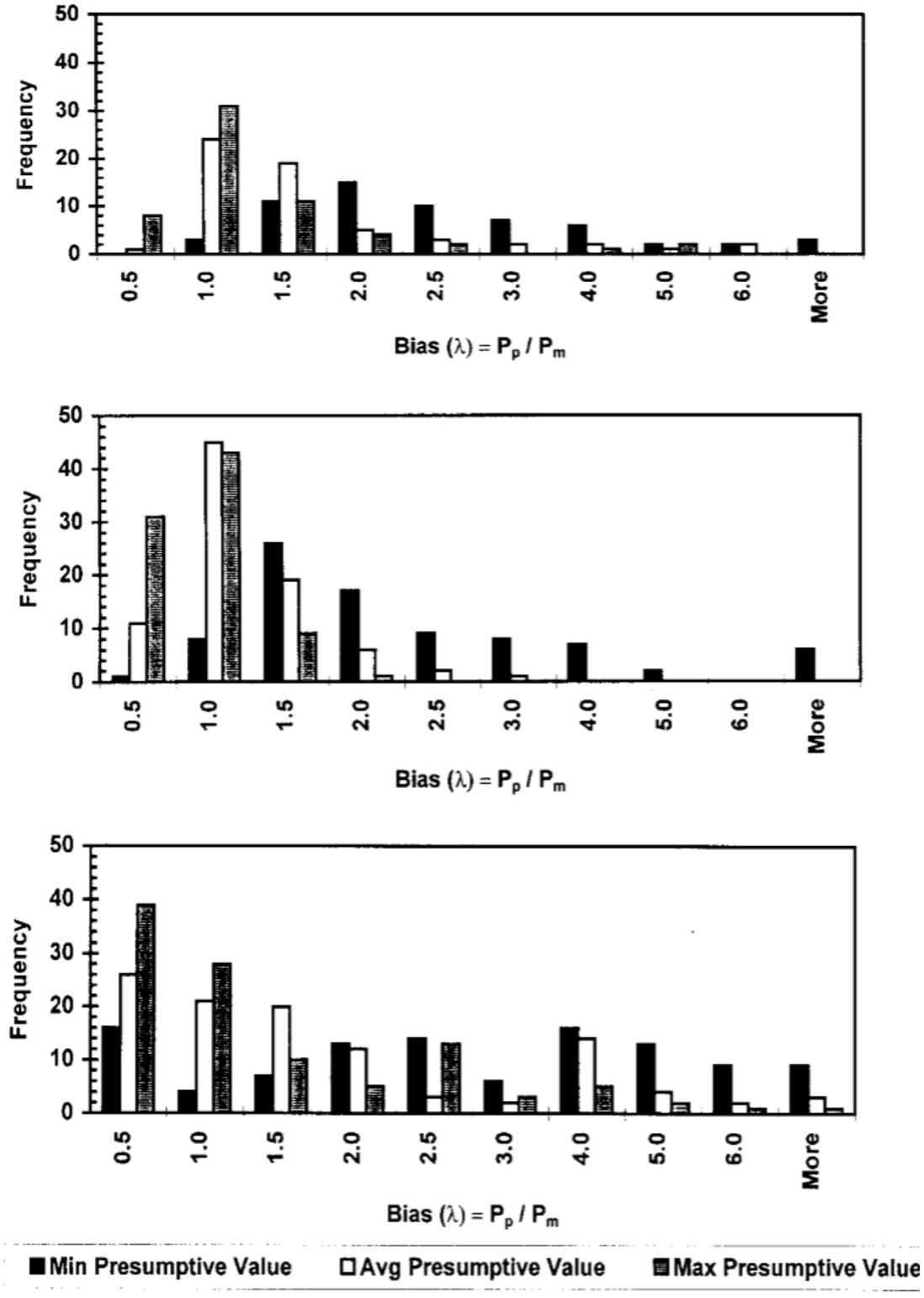

Figure 14 Histogram of bias factor of pullout resistance in (a) Clay (b) Sand (c) Rock

Table 11 Minimum factor of safety to ground / grout bond strength

Material	Bias (λ)	No. of Data	μ (λ)	COV (λ)	PF
Clay	P_m / P_p-min	59	2.56	0.71	0.05
	P_m / P_p-avg	59	1.48	0.75	0.42
	P_m / P_p-max	59	1.05	0.75	0.66
Sand	P_m / P_p-min	84	2.2	0.74	0.08
	P_m / P_p-avg	84	0.94	0.49	0.67
	P_m / P_p-max	84	0.63	0.47	0.88
Rock	P_m / P_p-min	107	3.13	0.81	0.19
	P_m / P_p-avg	107	1.70	0.97	0.44
	P_m / P_p-max	107	1.21	1.02	0.63

Basma (1991) employed a reliability-based design to compare the output of the classic proposed design of an anchored bulkhead with the output obtained by considering variability in soil parameters. Using the free-earth support method equations, Basma worked on two computer programs for cohesive soils and for granular soils. The outputs of these programs were statically analyzed using the "SAS" statistical program. This analysis leads to the development of design equations. These equations are mainly to facilitate the design process and to predict the means to study the variabilities of design outputs (See Figure 15). The minimum required safety factor that must be used for any given design parameter satisfying a required reliability, R, is estimated and plotted in a graph (see Figure 16). Two examples were employed to illustrate the use of all the equations. These examples allowed to evaluate the recommended factor of safety and it is indicated that the proposed factor of safety using the classical method is not always safe.

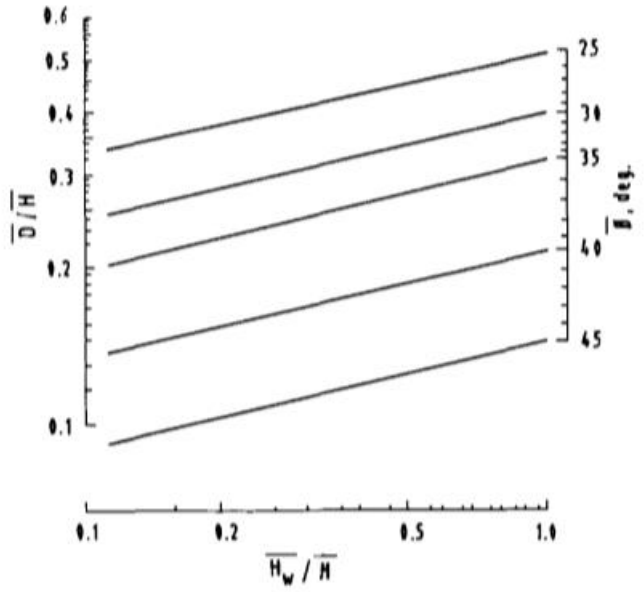

Figure 15 Determination of mean D/H with sand below dredge level

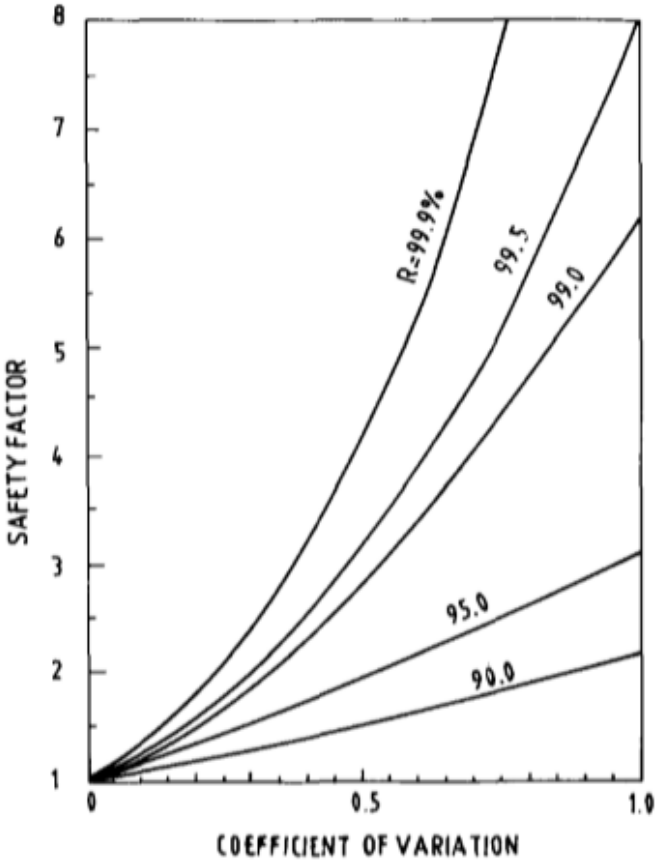

Figure 16 Minimum required safety factor for given reliability

Ching, Jianye, Hung-Jiun Liao, and Chia-Wei Sue (2008) investigated the ultimate capacities obtained from 46 pullout test results to calibrate the resistance factor of anchors in sandy and clayey soils. The nominal capacities were predicted to be compared with the actual capacities (See Figure 17). Based on this comparison, an uncertainty occurred in the relationship between these two capacities and it is indicated that the actual capacities are larger. Due to this uncertainty, a probabilistic approach was proposed to calibrate the resistance factor. Uncertain parameters were divided into 2 categories; uncertain soil parameters (friction angles φ, unit weights γ, the ratio between undrained shear strengths and effective vertical stresses β…) and uncertain model parameters (effective diameter which is replaced with enlargement factor ρ and decay parameter α). All the variables are considered to have lognormal distributions. Therefore, the calibration of the resistance factor was done after drawing the ρ_{new} and α samples with the Bayesian framework using the stochastic simulation (See Figure 18). A probabilistic analysis was done and the reliability factor was calculated to evaluate the code requirements. Moreover, in this study, some resistance factors are recommended for different design scenarios and for different target reliabilities (See Figure 19).

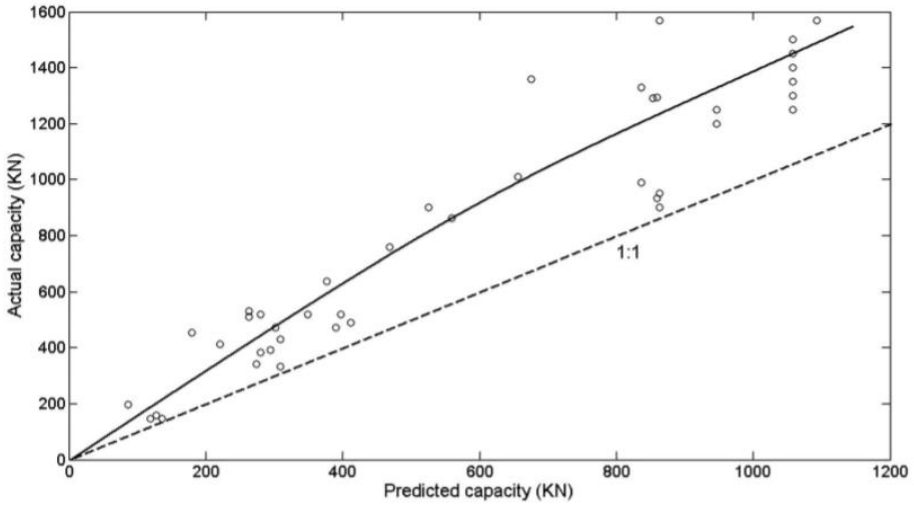

Figure 17 Actual versus nominal pullout capacities for anchors in database

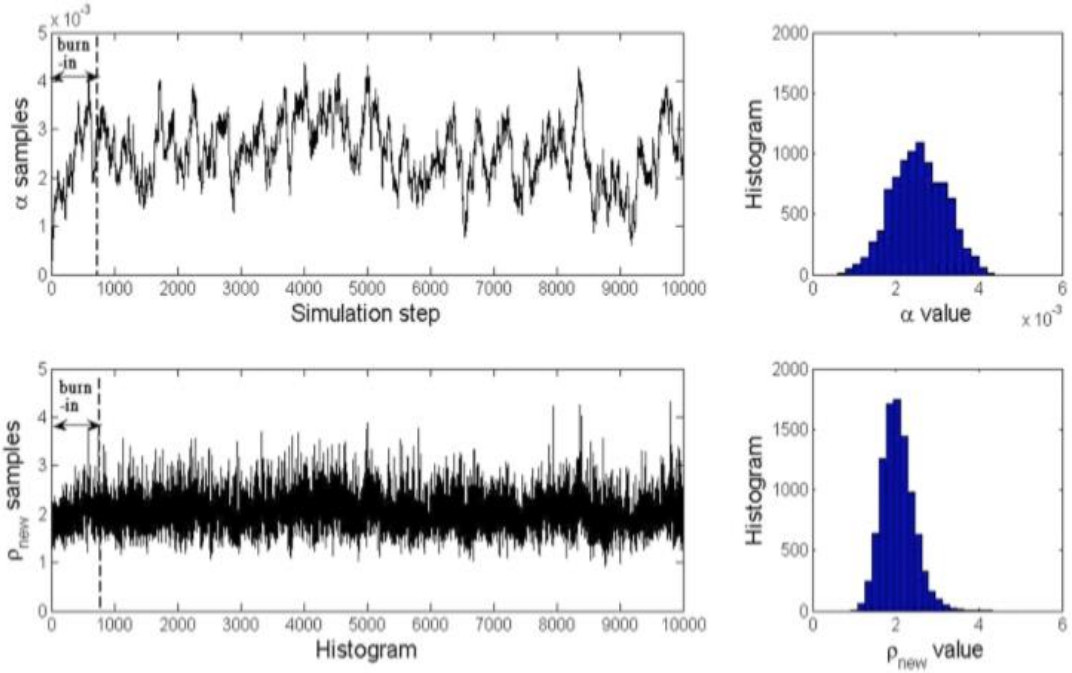

Figure 18 Markov Chain samples of α and ρ_{new} and corresponding histograms

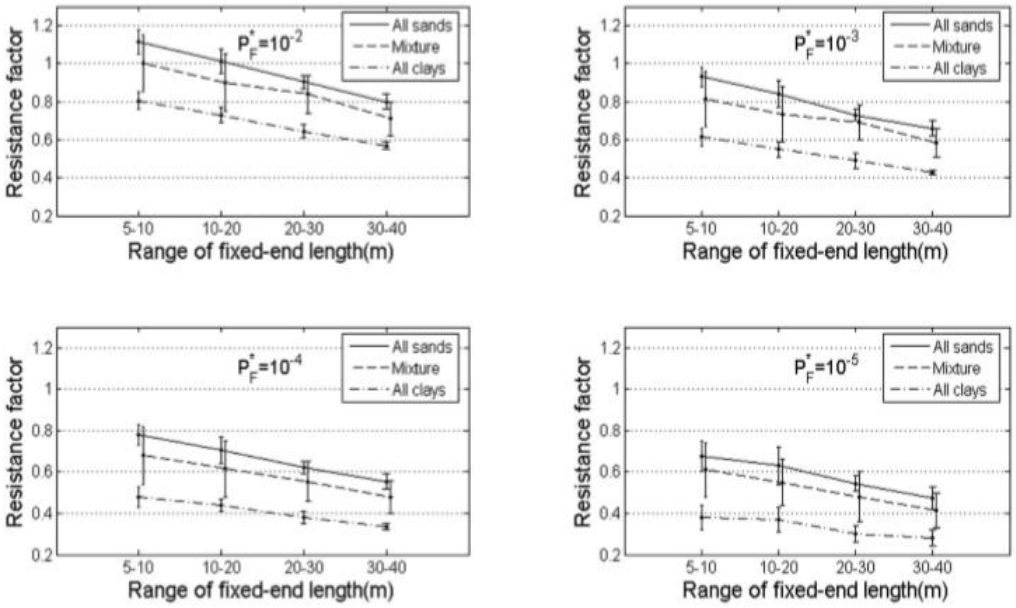

Figure 19 Recommended ranges of resistance factors for different design scenarios and target failure probabilities based on the existing data

Han, Jian-Yong, et al. (2017) discussed the design process of a deep excavation supported by tieback anchored pile walls in sandy soils using the China code and the European code. First, the design of the case study was done using the code used in China; the Technical Specification for Retaining and Protection of Building Foundation Excavations (JGJ 120-2012) (See Figure 20). The calculations were done using two methods: the classical method and the elastic method (see Table 12). For the latter analysis, the Deep Excavation software and the Finite Element Program are used. Also, additional calculations were done using the European code to provide a comparison between the two codes (See Figure 21). The comparison of these two codes was done based on a design example. The comparison indicated the common rules and the differences between the two codes. For the European code, the primary design theory is the reliability theory based on the limit states. While for the China code three design theories are used for different forms of design, that is, the reliability

theory based on the limit states, the design theory based on the allowable bearing capacity, and the design theory based on the safety factors. So we can say that the China code focuses on the design outcome while the European code focuses on the design procedure. Finally, according to the requirements of China and European codes, anchor tests were performed (see Figure 22). Based on the results, it is found that the anchors were initially locked, the anchor pre-stress had an exponential relationship with time. Also, there are three pre-stress loss stages: the fast loss stage, the slow loss stage, and the stable stage. In conclusion, the engineers should be aware of the fast loss stage.

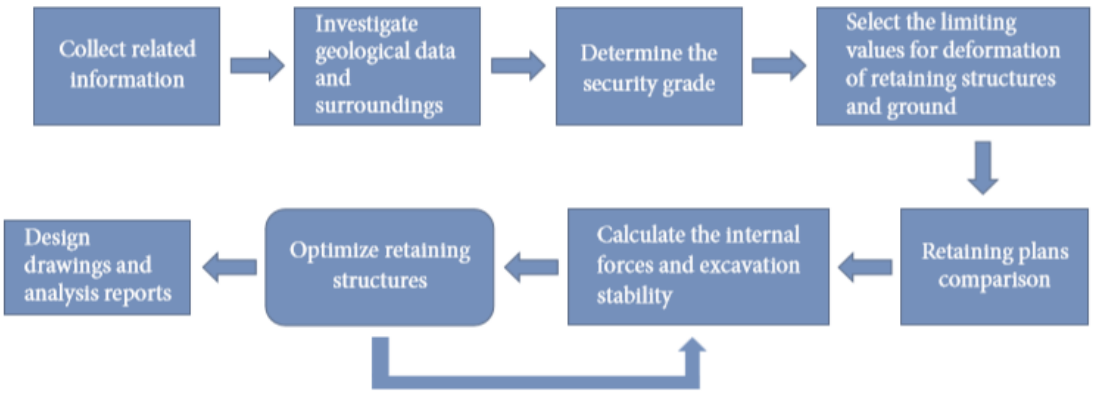

Figure 20 Design procedure for deep excavation in China

Table 12 Primary characteristics of classical method and elastic method.

Calculation method	Assumption of strut/anchor	Passive earth pressure	Pile stiffness	Calculation theory
Classical method	Hinged support	—	Ignored	Static equilibrium method, equivalent beam method, etc.
Elasticity method	Spring	Winkler elastic foundation	Considered	Beam on Winkler elastic foundation

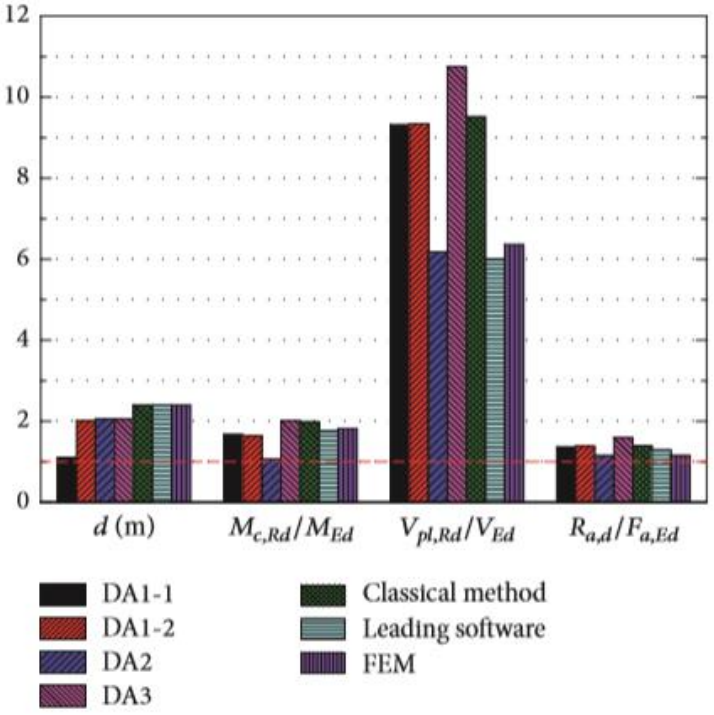

Figure 21 Design results obtained using various design approaches

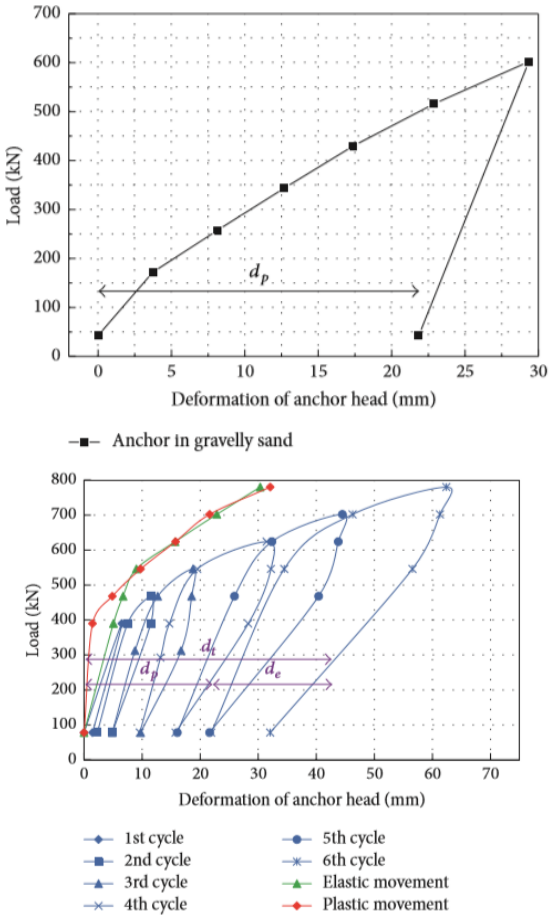

Figure 22 (a) Load-displacement response of the acceptance test. (b) Load-displacement response under cycle loading

CHAPTER 3
DATABASE COLLECTION

3.1 Introduction

Conventionally, the design of soil anchors is done using a deterministic approach. For calculating the bond strength, it is based on assuming a value for ultimate friction for the surrounding soil and a factor of safety. The predicted values of the ultimate friction may not be accurate. The most effective approach that can be used for the evaluation of this uncertainty is to study actual anchor test cases. This chapter represents details on real test cases which will be used to evaluate the uncertainty in the bonded zone.

3.2 Database

The database contains the results of 70 anchor tests in three geologic settings: 32 tests in Limestone, 26 in Marl, and 12 in Clay. The tests are executed in 28 different sites around Beirut. The baseline geological information available for Beirut was produced by Dubertret (1951) and indicates in its simplest representation two main geological units that dominate the geologic setting: A relatively young Miocene (m2b) stratum of Marl and Marly Limestone and an older and more significant Limestone sequence, the Cretaceous Sannine limestone (c4). The depths to which the Miocene stratum is present are variable and depend to a large degree on the faulting/uplift and erosion along the fault which bisects the central parts of the city in a roughly N-S direction. In some areas of the Beirut, more recent quaternary deposits of alluvial nature are present and form the majority of the soil cover wherever they exist. In other locations residual soils resulting from the decalcification of the marls form the upper

cover.

The database of anchor pullout tests is summarized in Table 13. In some sites, it is possible that anchors tests were conducted in two different geologic units depending on the elevation of the anchor that was tested. The main information that was available consisted of data of anchor head displacement versus applied pullout force. Information about each anchor included the bond length, free length, number of strands, and diameter of the drilled hole. In the majority of the cases analyzed, the anchors were installed using a hydraulic rig mounted on crawlers. The holes were drilled by rotary methods with flushing and installation of temporary steel casing. Immediately after drilling, the hole was grouted and anchor strands were lowered inside the hole. During the retrieval of the temporary casing, Type A grout was pumped to replace possible losses of grout which consists of Portland cement type 2 with cement to water ratio equals to 2, At least 24 hours after its first installation, grout type A was injected inside the pressure sleeved pipes. After the stoppage of injection, the grouting tube is flushed with clear water and the operation is resumed the following day until reaching the pressure criterion. After verifying its geometric positioning, the anchor is wedged in its final position until the setting of the grout. After installation, each anchor is tested after the sealed grout has reached the sufficient hardness.

The testing of anchors was executed relying on the general principles in French Norm NFP-94-153 and the interpretation was carried out per the guidelines established in the

"Recommendations TA95". The anchor test starts by positioning the anchor plate and connecting the multijacks to a single hydraulic power unit. During the loading stage, the load is applied in increments of 10% while measuring simultaneously the jack pressures and the elongation of the strands. The applied test load is maintained for 1

hour and the corresponding displacements are measured

Table 13. Data of Anchors

Test Number	Total Length (m)	Bond Length (m)	Free Length (m)	Number of Steel Tendons	Area of Steel (mm^4)	Inclination Angle (Degree)	Drilling Diameter (mm)	Hyperbolic Model Parameter a	Hyperbolic Model Parameter b	Type of Soil	Site
R400-P3	16	8	8	9	1350	30	140	5.87	0.84	Limestone	Site 1
R400-1	16	8	8	9	1350	30	140	17.75	0.85	Clay	Site 1
R400-2	16	8	8	9	1350	30	140	18.35	0.72	Marl	Site 1
R431-1	12	6	6	4	600	20	114	15.72	0.69	Marl	Site 2
R431-2	12	6	6	4	600	20	114	18.31	0.62	Marl	Site 2
R450-1	17.5	13.5	4	4	600	35	114	22.21	0.66	Clay	Site 3
R450-2	17.5	13.5	4	4	600	35	114	30.04	0.52	Clay	Site 3
R450-2G	17.5	13.5	4	4	600	35	114	30.45	0.51	Clay	Site 3
R482-1	10	5	5	4	600	20	114	3.07	0.93	Limestone	Site 4
R482-2	13	5	8	4	600	20	114	7.42	0.86	Limestone	Site 4
R482-3	13	5	8	4	600	20	114	15.25	0.74	Limestone	Site 4
R482-4	13	5	8	4	600	20	114	10.70	0.80	Limestone	Site 4
R482-5	13	5	8	4	600	20	114	11.65	0.82	Limestone	Site 4
R521-1	24	12	12	6	900	90	150	8.24	0.87	Marl	Site 1
R521-2	15	10	5	6	900	90	150	19.70	0.58	Clay	Site 1
R521-3	15	10	5	6	900	90	150	21.99	0.50	Clay	Site 1
R521-4	18	10	8	8	1200	90	150	7.76	0.92	Marl	Site 1
R521-5	18	10	8	8	1200	90	150	11.86	0.78	Marl	Site 1
R576-T42	16	8	8	4	600	35	114	18.26	0.63	Clay	Site 5
R595-1	10.5	5	5.5	3	450	20	114	29.31	0.51	Marl	Site 6
R595-2	10.5	5	5.5	3	450	30	114	23.96	0.66	Marl	Site 6
R595-3	11.5	6.5	5	4	600	20	114	17.74	0.67	Marl	Site 6
R598-1	11.5	5	6.5	5	750	20	130	15.65	0.74	Limestone	Site 7
R598-5	11	5	6	4	600	45	114	16.25	0.68	Marl	Site 7
R598-6	17	5	12	4	600	45	114	14.15	0.78	Marl	Site 7
R610-1A	10	5	5	4	600	20	114	26.57	0.85	Marl	Site 8
R610-1B	10	5	5	4	600	20	114	19.27	0.59	Marl	Site 8
R612-1	10	5	5	3	450	20	114	15.51	0.75	Marl	Site 9
R616-1	14	5	9	4	600	20	114	4.69	0.88	Limestone	Site 10
R656-1	10	5	5	5	750	20	114	11.26	0.76	Limestone	Site 11
R669-1	10	5	5	4	600	20	130	24.79	0.58	Limestone	Site 12
R669-2	10	5	5	4	600	20	130	6.57	0.89	Limestone	Site 12
R669-3	10	5	5	5	750	20	130	22.68	0.60	Marl	Site 12
R669-4	10	5	5	5	750	20	130	13.57	0.75	Limestone	Site 12
R675-1	10	5	5	4	600	20	130	25.34	0.56	Marl	Site 13
R675-2	10	5	5	4	600	20	130	17.38	0.71	Marl	Site 13

Table 13. (Continued) Data of Anchors

Test Number	Total Length (m)	Bond Length (m)	Free Length (m)	Number of Steel Tendons	Area of Steel (mm^4)	Inclination Angle (Degree)	Drilling Diameter (mm)	Hyperbolic Model Parameter a	Hyperbolic Model Parameter b	Type of Soil	Site
R675-3	10	5	5	4	600	20	130	18.56	0.71	Limestone	Site 13
R675-4	10	5	5	4	600	20	130	10.32	0.82	Limestone	Site 13
R682-1	10	5	5	5	750	20	130	7.46	0.87	Limestone	Site 14
R682-2	10	5	5	5	750	20	130	39.40	0.33	Limestone	Site 14
R682-3	10	5	5	5	750	20	130	12.60	0.77	Limestone	Site 14
R682-4	10	5	5	5	750	20	130	50.39	0.21	Marl	Site 14
R682-5	16.5	5	11.5	5	750	20	130	5.50	0.89	Limestone	Site 14
R705-1	10	5	5	5	750	20	130	30.21	0.51	Limestone	Site 15
R705-2	10	5	5	5	750	20	130	50.96	0.18	Marl	Site 15
R707-1	10	5	5	5	750	20	130	20.85	0.66	Limestone	Site 16
R707-2	10	5	5	5	750	20	130	49.89	0.12	Marl	Site 16
R707-3	10	5	5	5	750	20	130	20.58	0.31	Marl	Site 16
R721-1	10	5	5	5	750	33	130	13.69	0.72	Limestone	SiIe 17
R724-1	10	5	5	4	600	33	130	25.40	0.55	Marl	Site 18
R724-2	10	5	5	4	600	24	130	21.91	0.63	Clay	Site 18
R725-1	10	5	5	5	750	33	130	9.69	0.83	Limestone	Site 19
R746-1	10	5	5	4	600	30	130	25.99	0.58	Limestone	Site 20
R746-2	10	5	5	4	600	30	130	9.22	0.84	Limestone	Site 20
R749-2	13	8	5	3	450	30	130	19.71	0.67	Clay	Site 21
R751-1	15	10	5	5	750	20	130	31.19	0.51	Clay	Site 22
R751-2	13	8	5	3	450	20	130	14.26	0.76	Clay	Site 22
R761-1	11	5	6	5	750	20	130	20.68	0.67	Limestone	Site 23
R761-2	11	5	6	4	600	20	114	5.98	0.88	Limestone	Site 23
R761-4	10	5	5	4	600	20	114	28.44	0.52	Limestone	Site 23
R764-1	10	5	5	4	600	20	114	8.61	0.86	Marl	Site 24
R764-2	10	5	5	4	600	20	130	15.70	0.76	Limestone	Site 24
R768-1	10	5	5	4	600	20	130	13.70	0.77	Marl	Site 25
R768-4	10	5	5	4	600	20	130	19.44	0.87	Marl	Site 25
R768-5	15	10	5	5	750	20	130	28.42	0.51	Clay	Site 25
R769-1	12.5	5	7.5	4	600	20	130	9.33	0.85	Limestone	Site 26
R769-2	12.5	5	7.5	4	600	20	130	12.86	0.79	Limestone	Site 26
R787-1	16	6	10	4	600	20	114	18.53	0.74	Limestone	Site 27
R787-2	12	6	6	4	600	20	114	15.21	0.71	Marl	Site 27
R788-1	11.5	5	6.5	3	450	20	114	34.56	0.43	Limestone	Site 28

CHAPTER 4 ASSESSMENT OF UNCERTAINTY IN THE DISPLACEMENT IN THE BONDED ZONE

4.1 Introduction

The basic idea from this section is to quantify the uncertainty in the displacement in the bonded zone obtained from the anchor tests. A probabilistic model based on anchor tests data is proposed to describe the nonlinear load-displacement curves of the anchor in different soil types.

4.2 Analysis of Test Results

The raw data from each anchor test consists of the applied load (T) versus the measured total anchor displacement (Δ). The first step in the analysis consists of calculating the average bond stress in the grouted zone (F_b) for each load increment using Equation (1):

$$f_b = \frac{T}{\Pi\, D\, Lb} \qquad (1)$$

Where: f_b = the average stress in the bonded length (kN/m^2), T = the load applied on the anchor during the test (kN), D = drilled hole diameter (m), and L_b = bonded length (m). Data showing the average bond stress versus total anchor displacement is presented in Figure 23 for example cases involving anchors in limestone, marl, and clay, respectively. The results indicate total measured anchor displacements ranging from 70mm (limestone) to 120mm (clay) for the cases shown in Figure 23. Since part of the total measured displacement is attributed to elongation in the steel strands in the free length (Δ_f), this elastic elongation was subtracted from the total measured displacement to

determine the average slip of the anchor in the bonded zone. The calculated slip in the bonded length (D_b) is calculated from Equations (2) and (3) such that:

$$\Delta_b = \Delta - \Delta_f \quad (2)$$

$$\Delta_f = \frac{T\,L_f}{E\,A} \quad (3)$$

Where: Δ_b = the slip in the bonded length (mm), Δ = total anchor head displacement (mm), Δ_f = the displacement in the free length (mm), L_f = free length (mm), E = modulus of elasticity of the steel strands (20 x 10^8 kPa), and A = area of the steel strands (m^2). Figure 23 shows the curves relating the average bond stress versus the predicted slip/displacement in the bonded zone. As indicated in the figure, a significant portion of the total anchor displacement is attributed to elongation of strands in the free length of the anchor.

Figure 24 shows the variation of the average stress in the bonded zone as a function of the predicted anchor slip/displacement in the bonded zone for all the tests in the three types of soil in the database. Results on Figure 24 indicate that the bond stress – displacement curves for anchors in a given geologic unit form groups that can easily be distinguished based on the observed response. As expected, the curves representing anchors in limestone exhibit a relatively stiffer stress-displacement response, compared to anchors in marl, which in turn show a stiffer response compared to anchors in clay. It is also clear that even in the same geologic unit, the curves exhibit a significant degree of variability in the response due to variability in soil/rock properties, construction related factors, and properties of the grout.

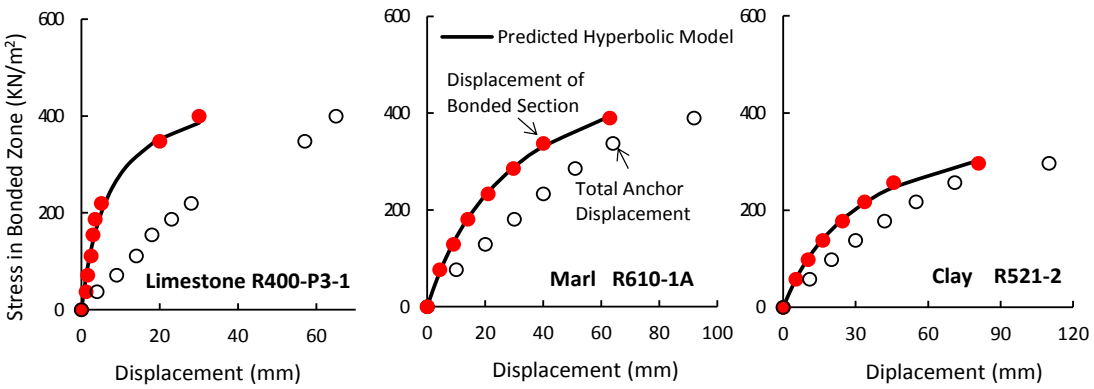

Figure 23. Example Results from Pullout Tests in limestone, marl, and clay

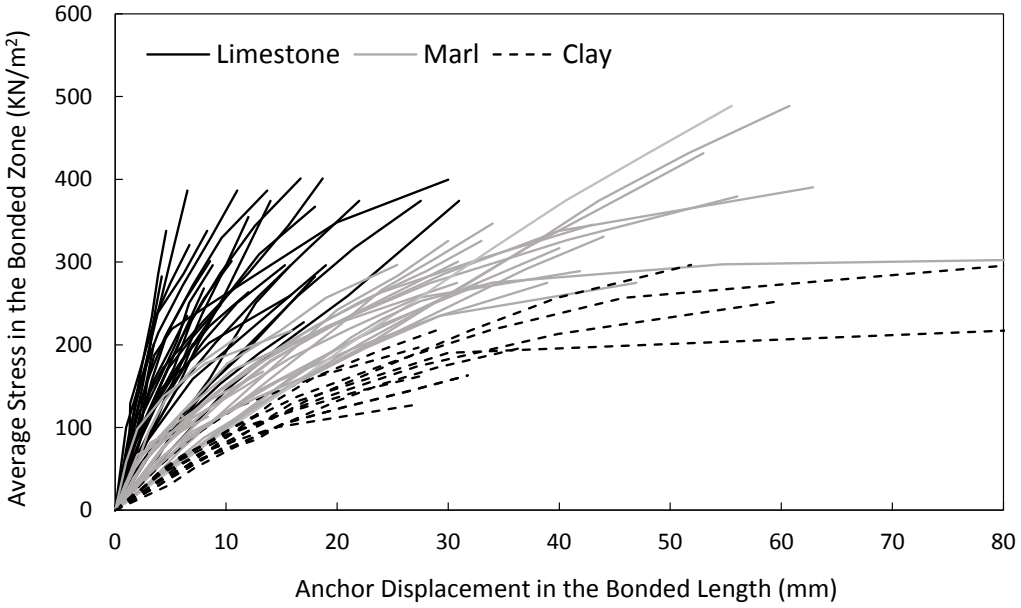

Figure 24. Variations of the Average Stress in the Bonded Zone as a Function of Displacement in the Bonded Zone for All the Tests

4.3 Probabilistic hyperbolic load-settlement model

4.3.1. Objective and background

The main objective of doing a probabilistic hyperbolic load-settlement model is to quantify the variability in the observed response. This is achieved by using a hyperbolic model to fit the observed relationship between the average stress and anchor slip in the bonded zone. The hyperbolic model is a 2-parameter model that has been previously used to fit load-displacement relationships for problems involving piles (examples Phoon et al. 2006, 2007; Dithinde et al. 2011; Stuedlein and Uzielli 2014;

Reddy and Stuedlein 2017; Tang and Phoon 2018a-c) and shallow foundations (Uzielli and Mayne 2011; Huffman and Stuedlein 2014; Najjar et al. 2014, 2017).

4.3.2. Methodology

In the hyperbolic model, the response is captured by 2 parameters "a" and "b", where "a" represents the initial slope and "b" represents the asymptotic value of the normalized load-settlement curve. In the hyperbolic model, the applied load/stress is usually normalized by the "ultimate/maximum" load/stress prior to fitting the curve to the observed response. In the problem at hand, the hyperbolic relationship is presented in Equation (4) and links the normalized stress in the bonded zone to the average predicted anchor slip in the bonded zone such that:

$$\frac{f_b}{f_{b,max}} = \frac{\Delta_b}{a+b\Delta_b} \quad (4)$$

Where $f_{b,max}$ is the ultimate bond stress. Given that the ultimate bond stress was not reached in many of the anchor tests available in the database, ultimate bond stresses that were consistent with common design practice/experience for anchors in Beirut were adopted to normalize the data presented in Figure 2. Accordingly, $f_{b,max}$ was assumed to be equal to 600 kPa for anchors in limestone, 350 kPa for anchors in marl, and 250 kPa for anchors in clay. Exceptions to these assumptions included: (1) two tests in limestone where a reduced $f_{b,max}$ of 400 kPa was adopted due to the fact that the anchor tests approached failure at these values, and (2) three tests in marl, where a higher $f_{b,max}$ of 500 kPa was adopted given that the geology was classified as "marly limestone" rather than "marl".

Following the normalization of the data shown in Figure 24, two parameter hyperbolic models having the mathematical form presented in Equation (4) where fit to each test using linear regression.

4.3.3. Analysis and Results

The resulting a and b parameters for each test were calculated and presented in Table 14. As expected, the uncertainty in the observed stress-displacement curves was translated clearly in the variability in the resulting values of a and b within a given geologic unit. The statistics representing the uncertainty in a and b for each geologic unit were calculated and presented in Table 14.

Table 14. Statistical Parameters of the hyperbolic bond stress – bond displacement relationship

	Limestone		Marl		Clay	
Statistics	a	b	a	b	a	b
Mean	15	0.74	21.8	0.63	23	0.61
Standard Deviation	9.09	0.14	11.57	0.21	5.66	0.11
Coefficient of Variation	0.61	0.19	0.53	0.33	0.25	0.18
Beta Parameter, a	3	0	7	0	14	0.5
Beta Parameter, b	40	0.91	50	0.92	32	0.85
Beta Parameter, m	-3.46	5.63	-3.46	3.16	-0.88	-4.53
Beta Parameter, s	4.25	3.86	4.45	4.21	5.32	5.67
Correlation Coefficient	-0.99		-0.87		-0.79	

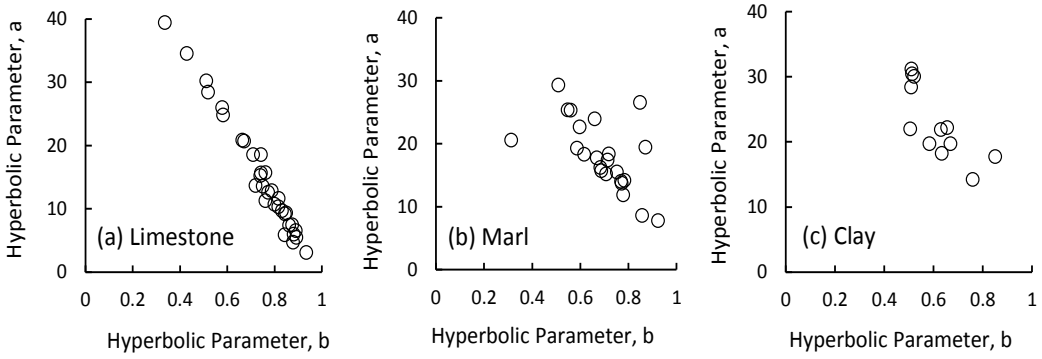

Figure 25. Relationship between the two hyperbolic model parameters from the anchor tests

The results in Table 14 indicate that the parameter "a" seems to be more uncertain than parameter "b", particularly for cases involving anchors in limestone and marl, where coefficients of variation as high as 0.61 are recorded for "a" compared to 0.33 for "b". The parameters for anchors in clay show the least variability with coefficients of variation as low as 0.25 for "a" and 0.18 for "b". Interestingly, a plot showing the relationship between parameters a and b (Figure 25) for each geologic unit indicates that the parameters are highly correlated negatively with correlation coefficients as high as -0.99 for anchors in limestone and -0.79 for anchors in clay. Negative correlations between hyperbolic model parameters have been reported in many published studies for piles and shallow foundations.

4.3.4. Determination of Hyperbolic Parameters Distributions

To complete the statistical model for the hyperbolic parameters that model the relationship between the anchor bond stress and anchor slip in the bonded zone, candidate probability distributions were tested against the observed data for a and b. These include the conventional lognormal probability distribution in addition to a more general four-parameter beta distribution that is bounded in an interval [a b]. The beta distribution is based on a transformation (Equation 5) from a standard normally distributed random variable G, into a random variable X that is bounded on the interval a to b such that:

$$X = a + \frac{1}{2}(b-a)\left[1 + tanh\left(\frac{m+sG}{2\pi}\right)\right] \qquad (5)$$

Where m, s, a and b are the location, scale, lower bound and upper bound parameters, respectively. The probability density function of the bounded distribution of X is:

$$f_X(x) = \frac{\sqrt{\pi}\,(b-a)}{\sqrt{2s}(x-a)(b-x)} * exp\left\{-\frac{1}{2s^2}\left[\pi \ln\left(\frac{x-a}{b-x}\right) - m\right]^2\right\} \quad (6)$$

The 4-parameters of the bounded distribution were calibrated to produce a cumulative distribution function (CDF) that best fits the observed CDF of the data. The calibration was conducted in "Microsoft Excel" through the Solver tool that allows for solving the optimization problem in which the 4 parameters of the bounded distributions were obtained.

Figure 26 shows the observed CDFs for a and b in the different geologic units and the theoretical lognormal and beta distributions that were used to model the variability in the hyperbolic parameters. The four parameters that describe the beta distributions shown in Figure 26 are presented in Table 2 for the cases of anchors in limestone, marl, and clay. Results on Figure 26 show that the four parameter beta distribution provides a more realistic representation of the uncertainty in a and b for almost all of the cases analyzed. This distribution, along with the correlation coefficients shown in Table 14, can be used to model the joint probability density functions representing the uncertainty in the hyperbolic models for the anchor tests that were analyzed in this study.

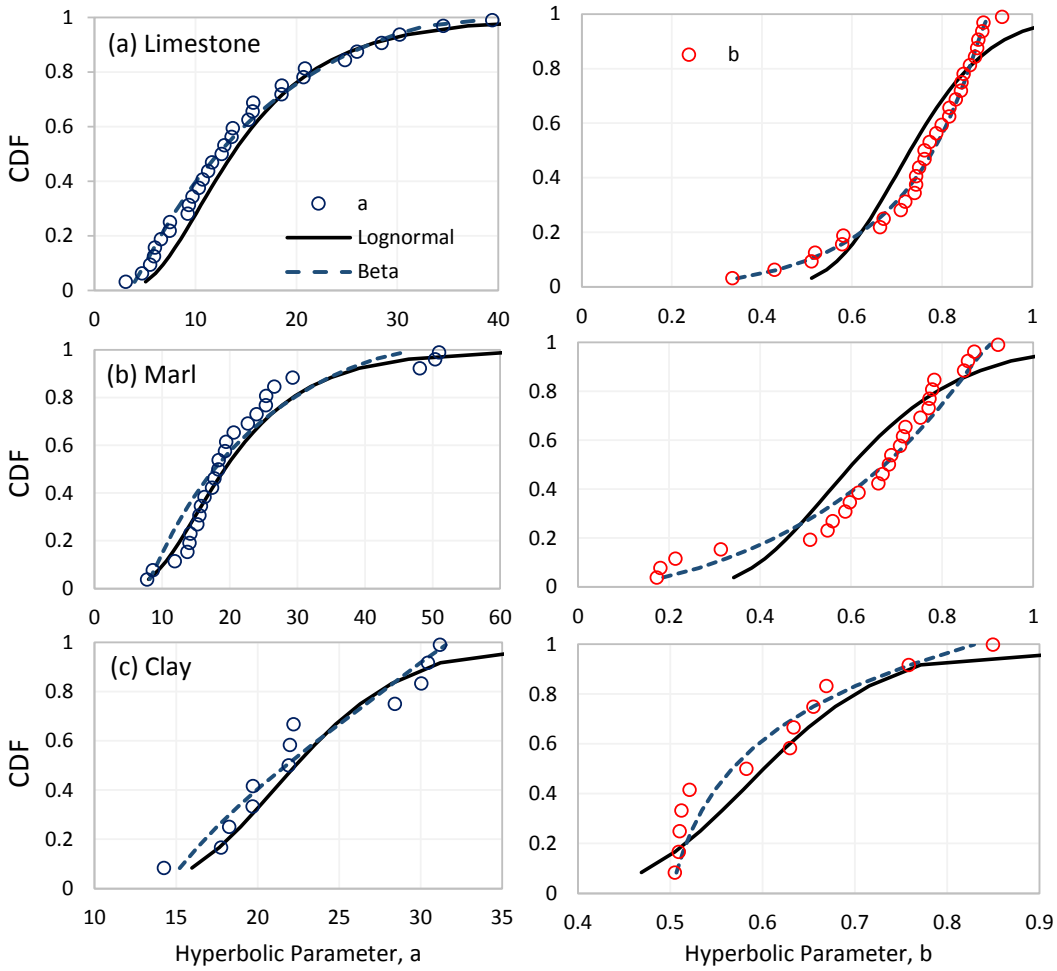

Figure 26. Actual and Theoretical Lognormal and Beta Distributions for Modeling the Uncertainty in the Hyperbolic Model Parameters for Anchors

4.4 Monte Carlo Simulations

Monte Carlo Simulations are used in order to check if the obtained model reflects the available data. Two main parameters, which illustrate the uncertainty in the displacement in the bonded zone, are considered as random variables. These parameters are the hyperbolic parameters, a and b. After determining the distribution of a and b in the previous section, they are modeled as Beta distributed random variables for simulations. Monte Carlo simulations generate numerous estimations of a and b which will be compared later to a and b values obtained from the existing data. For each type of soil, 100 a – b pairs are simulated. To make the comparison, the 100 simulated a – b

values are transformed into 100 curves using equation (4) and compared with the existing curves.

Figure 27 represents the curves obtained from Monte Carlo simulations and those that are obtained from the tests. These curves represent the variation of the average stress in the bonded zone as a function of the anchor displacement in the bonded zone in Limestone, Marl, and Clay.

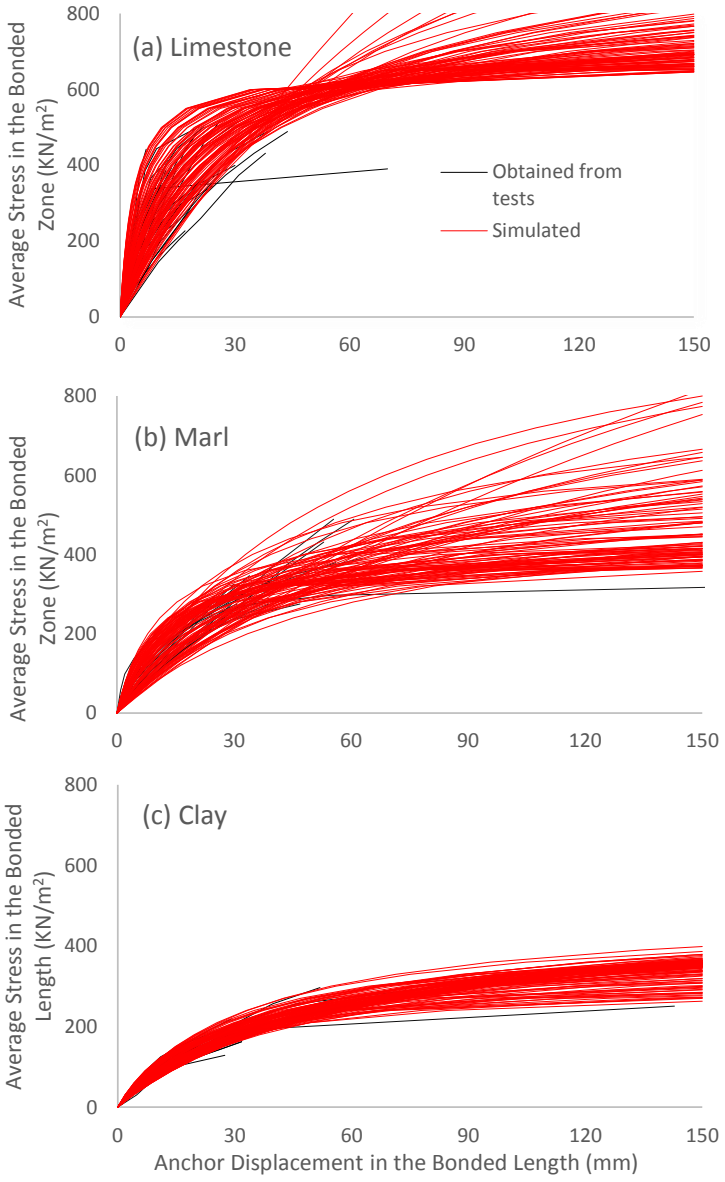

Figure 27 Comparison between the average stress in the bonded zone as a function of the anchor displacement in the bonded length curves obtained from simulation and the curves obtained from tests

CHAPTER 5
DESIGN EXAMPLE

5.1 Introduction

In this chapter, a design example for an anchored retaining wall is presented to show the practical use of the discussed model in chapter 4. This example aims to associate the deterministic analysis of an anchored retaining wall with the probabilistic analysis of the wall. This example is modeled using Wallap. This software, which is commonly used by engineers to design anchored retaining walls, does not take into consideration the displacement in the bonded zone. The resulted model from chapter 4 will help estimate the displacement in the bonded zone, which will be used later to calculate the probability of failure of the wall.

5.2 Background

Wallap is a specialized geotechnical computer software to analyze shoring walls and horizontally loaded piles. It is based on the analysis of shoring walls using the beams on the elastic foundation (BEF) method.

Retaining walls are normally designed against earth pressure. This is why the earth pressure coefficients are computed by Wallap, to be used in the earth pressure analysis. Wallap treats the wall model at all its construction stages. It determines wall deformations, anchor working loads, and shear stresses as well as moments at each stage.

5.3 Wallap Models

Three anchored retaining walls are modeled on Wallap to support an excavation of two-layered soil of 7 meters. The design of the anchored wall is assumed to be the same in the three cases. The different in each case is the type of the soil's second layer. In the first case, the soil is constituted of a top layer of silty sand and a layer of Limestone underneath it. Under the silty sand layer of the second case, there is a layer of Marl, while in the third case there is a layer of Clay. In the three cases, the anchor is bonded in the second layer. Each case is modeled two times. In the second time, the value of half of the anchor's bonded length is added to the free length of the anchor which is a method used by a lot of engineers during the design phase.

5.4 Input Parameters

The main input parameters are divided between soil layers, soil types, groundwater level, wall or pile, anchors (struts), surcharge, stages and, the factor of safety.

5.4.1. Soil layers

Soil layers are defined by their name and their elevation in this section. The used soil layers and their elevations for each case are summarized in table 15.

Table 15 Soil Layers

Case	Soil Layer	Elevation (m)
1	Silty Sand	0
	Limestone	-5.5
2	Silty Sand	0
	Marl	-5.5
3	Silty Sand	0
	Clay	-5.5

5.4.2. Soil Types

Each layer is defined by its bulk density, type (cohesive/non-cohesive), drained or undrained analysis, normally or over-consolidated, cohesion, soil modulus Poisson's ration and, the angle of friction to calculate earth pressure coefficient at rest, active and, passive earth pressure coefficients. All the soil parameters are summarized in table 16.

Table 16 Soil Parameters

Soil Layer	Silty Sand	Limestone	Marl	Clay
Bulk Unit Weight (kN/m^3)	18	22	20	19
Soil Type	Cohesionless	Cohesive	Cohesive	Cohesive
Consolidation State	OC	OC	OC	OC
Drained/Undrained	-	Drained	Drained	Drained
Angle of Friction (Degree)	30	30	25	15
Coefficient of Earth Pressure at Rest, K_0	0.5	0.577	0.577	0.74
Active Earth Pressure Coefficient, K_a	0.333	0.333	0.406	0.569
Passive Earth Pressure Coefficient, K_p	3	3	2.464	1.698
Drained Cohesion (kN/m^2)	-	60	40	30
Young's Modulus (kN/m^2)	12500	230000	100000	50000
Poisson's Ratio	0.333	0.2	0.25	0.4

5.4.3. Groundwater Conditions

In the studied cases, the groundwater is considered to be under the excavation. So, it has no effect on the three cases.

5.4.4. Retaining Wall

The retaining wall consists of a pile wall. All the wall characteristics are summarized in table 17

Table 17 Pile's Characteristics

Pile Diameter (m)	0.6
Pile Spacing (m)	1.8
Elevation of Toe of Wall (m)	-10
Young's Modulus (kN/m^2)	23000000
Moment of Inertia per Unit Length (m^4/m)	0.00353

5.4.5. Anchors (Struts)

For the three cases, the same one-row anchors are employed. For each case, two different free lengths are executed. One of them is the original free length, which is designed so that the bond zone is below the sliding surface. The second free length is taken to be equal to the free length + 0.5 x bond length. The bonded length is predicted considering a factor of safety equals to 2 using equation (7). All the details about the anchors are shown in table 18.

$$L_b = \frac{C}{\Pi \, x \, De \, x \, fb \, ,max} \qquad (7)$$

Where C is the anchor capacity (kN),

Table 18 Anchors Characteristics

Soil Type	Limestone	Marl	Clay
Anchor Elevation (m)	-2	-2	-2
Anchor Spacing (m)	2.4	2.4	2.4
X-section Area of Anchor (m^2)	0.0006	0.0006	0.0006
Young's Modulus (kN/m^2)	200000000	200000000	200000000
Free Length (m)	7	7	7
Free Length + 0.5 Bonded Length (m)	9	10	11.5
Strut Inclination (Degree)	30	30	30
Pre-stress (kN)	300	300	300

5.4.6. Surcharge

The surcharge is applied on the ground level and it is taken to be equals to 15 kN/m^2

5.4.7. Factor of Safety

The Factor of safety for the wall is taken equals to 1.5.

Figures 28, 29 and 30 illustrate the three executed cases.

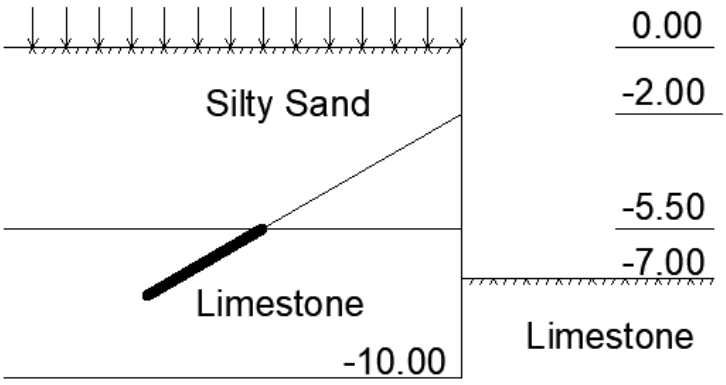

Figure 28. Anchored Wall in Case 1 (Limestone)

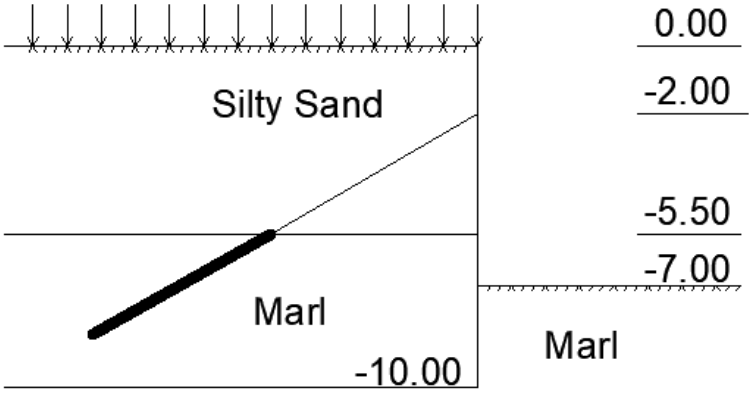

Figure 29. Anchored Wall in Case 2 (Marl)

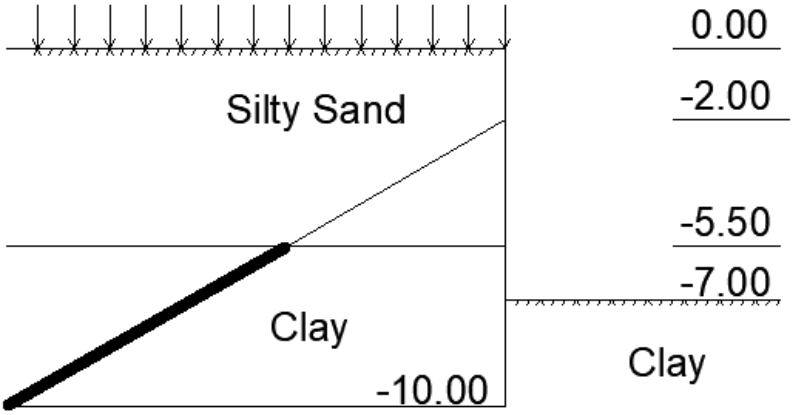

Figure 30. Anchored Wall in case 3 (Clay)

5.5 Results

Considering the results of Wallap, the main focus is on the working load of the anchors, the displacement at the top of the wall, and the displacement at the level of the anchor. The working load is used to calculate the friction that is used later for the Monte Carlo simulations in order to compute the probability of failure. The displacement at the top of the wall is taken as the maximum displacement of all the stages. Then, it is checked to assure it is less than the allowable displacement which, in this case, is 2cm or around it. While the displacement at the level of the anchor is taken from stage five (the first stage is not considered since the anchor is not installed yet). This displacement is basically the displacement in the free zone of the anchor and it is used to compute the displacement in the bonded zone and the total displacement using the obtained model for each type of soil.

Figure 31 represents the displacement of the retaining wall as a function of the level for case 1, case 2 and, case 3. Diagram (a) represents the envelope of all the stages while diagram (b) represents the displacement at stage 5. Tables 19, 20 and, 21 summarizes all the results of the three cases.

Comparing the three cases, the displacement of the anchored wall in the Limestone is lower than the displacement in the two other cases. In the case of the wall in the Clay, the displacement is the highest.

For each case, increasing the free length involves more displacement except for the Limestone case where no apparent change in the displacement is shown.

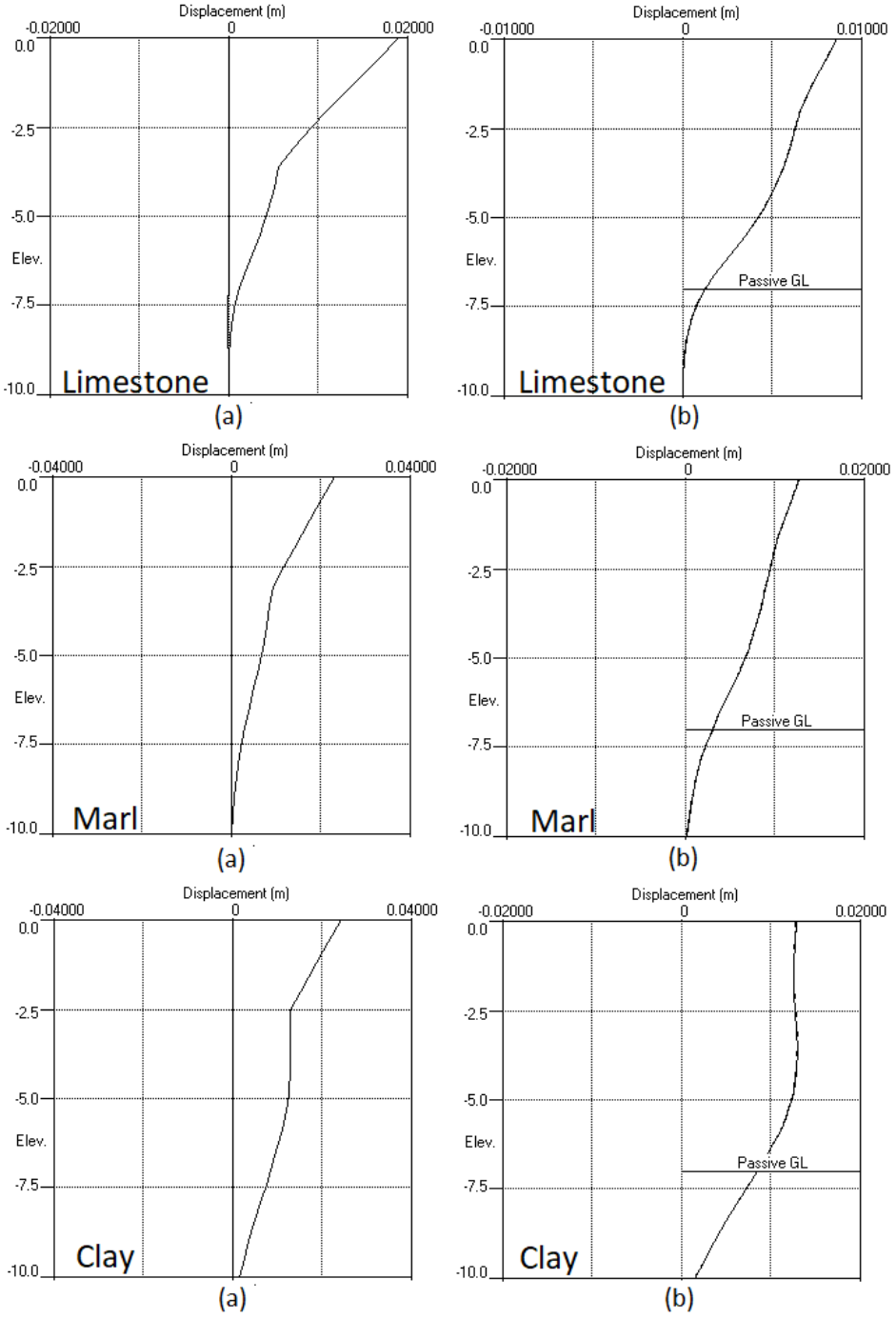

Figure 31.Displacement Diagram form Wallap: (a) Envelope of all stages of displacement of the wall. (b) Displacement of the wall at level 5.

Table 19. Results of case 1

	Level	Total Displacement (mm)
envelope	at the top of the wall	19
Stage 5 - Lf = 7m	at the level of the anchor	7
	at the top of the wall	9
Stage 5 - Lf+0.5 Lb = 9m	at the level of the anchor	7
	at the top of the wall	9

Table 20. Results of case 2

	Level	Total Displacement (mm)
envelope	at the top of the wall	23
Stage 5 - Lf = 7m	at the level of the anchor	10
	at the top of the wall	13
Stage 5 - Lf+0.5Lb = 10m	at the level of the anchor	11
	at the top of the wall	14

Table 21. Results of case 3

	Level	Total Displacement (mm)
envelope	at the top of the wall	24
Stage 5 - Lf = 7m	at the level of the anchor	13
	at the top of the wall	13
Stage 5 - Lf+0.5Lb = 11.5m	at the level of the anchor	14
	at the top of the wall	14

5.6 Determination of the Displacement in the Bonded Zone Distributions

In order to figure out the distribution of the displacement in the bonded zone, Monte Carlo simulations are used. The discussed model in chapter 4 and the displacement at the level of the anchor, which is the displacement in the free zone, are used to compute

the displacement in the bonded zone. Then, the total anchor displacement is computed by adding to the displacement in the bonded zone the displacement in the free zone obtained from Wallap. Ten thousand Monte Carlo simulations are generated for a and b where a and b are treated as Beta variables. Using these values, the displacements in the bonded zone are calculated. The means, the standard deviations and the coefficients of variations of the displacement in the bonded zone and the total displacement are represented in table 22.

The probability distribution of the displacement in the bonded zone is tested and compared with theoretical probability distribution functions. These distribution functions include the normal distribution, the lognormal distribution, and beta distribution. The CDFs of the displacement in the bonded zone obtained from the simulations and the theoretical normal, lognormal and, beta distributions are displayed in Figure 32.

The results in Figure 32 indicate that the probability distribution that can be used to fit the displacement in the bonded zone is the beta distribution.

Table 22. Statistical Parameters of the Bonded Zone Displacement

	Limestone		Marl		Clay	
	Displacement in the bonded zone (mm)	Total displacement at the level of the anchor (mm)	Displacement in the bonded zone (mm)	Total displacement at the level of the anchor (mm)	Displacement in the bonded zone (mm)	Total displacement at the level of the anchor (mm)
Mean	5.54	12.54	8.89	18.89	9.84	22.84
Standard Deviation	2.90	2.90	3.71	3.71	2.03	2.03
COV	0.523	0.231	0.418	0.197	0.207	0.089

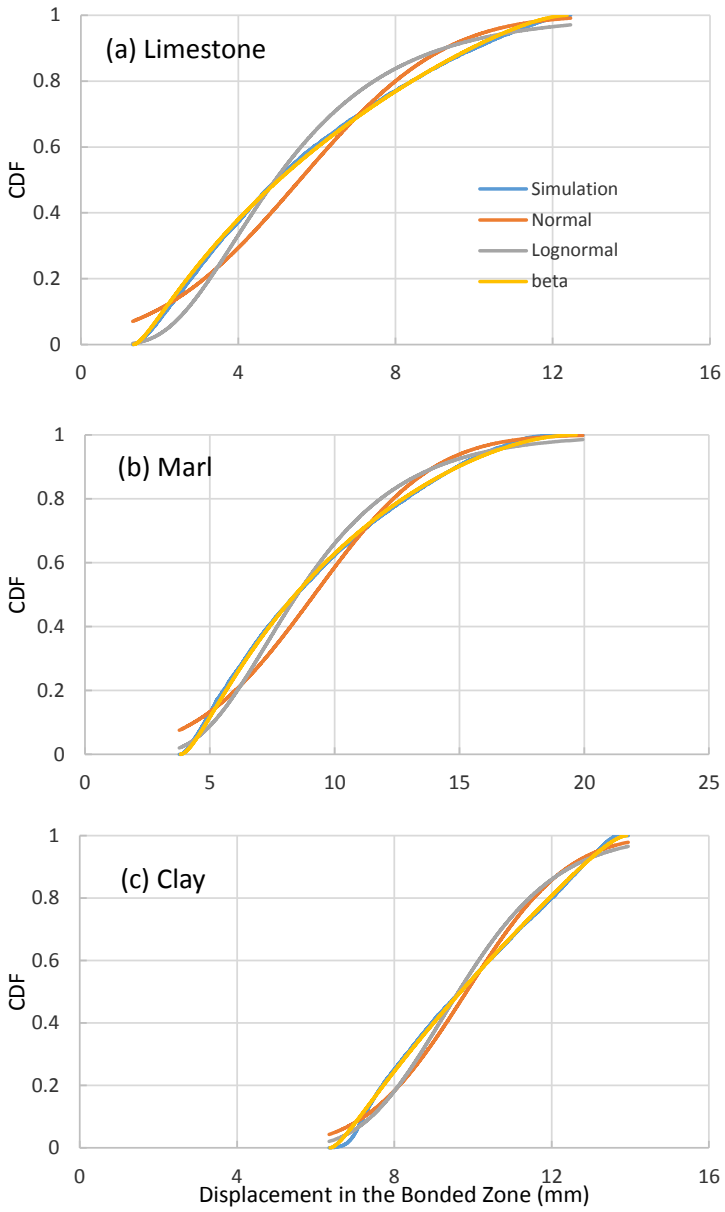

Figure 32. Actual and Theoretical Normal, Lognormal, and Beta Distributions for Modeling the Uncertainty in the Bonded Zone Displacement

5.7 Reliability-Based Design

The reliability-based design considers the sources of uncertainty that can affect the design decisions. Also, it relies on the probability of failure to detect and avoid design errors. The probability of failure approach requires the precision of allowable displacement. The total anchor displacement that is computed in the previous section is

used to compute the probability of failure of the anchored wall. The failure is defined when the displacement exceeds a certain allowable value. The probability of failure is calculated for several different levels of allowable displacement but only one allowable displacement is considered in this case which equals to 2cm. The resulted probabilities of failure for the three cases are displayed in table 23. The probability of failure should be tested if it is acceptably small. Usually, two ranges are considered acceptable for the probability of failure depending on the studied case; 0-5% and 5-10%. Based on the results in table 23 and considering the 2cm allowable displacement, it is shown that the probability of failure of the wall in Marl and Clay are unacceptably high. On the other hand, it is too conservative in the case of Limestone. To adjust these probabilities, a redesign is required. The design of the anchored wall is repeated while changing the spacing between the anchors. All the results for different anchor spacing are shown in table 24. Considering that the 0 – 5% is the acceptable range, the anchors, in the case of Limestone, should be at a spacing of 2.8m, while in the case of Marl and Clay it should be at 1.6m. On the other hand, for the 5-10% range, the anchor spacing, in case of limestone, should be increased to 3m. While in the case of Marl and Clay, the anchor spacing should be decreased respectively to 1.7m and 1.8m. Figure 33 represents the variation of the anchors spacing in each case for the two probabilities of failure 5% and 10%.

Table 23. Probability of Failure of the Anchored Wall for the Three Cases for Different Levels of Allowable Displacements

	Limestone	Marl	Clay
P (S > 1cm)	76.1	100	100
P (S > 1.5cm)	22.64	85.09	100
P (S > 2cm)	**0**	**34.8**	**95.45**
P (S > 2.5cm)	0	8.56	20.13

Table 24. Probability of Failure at Different Anchor Spacing

	Limestone								
Anchor Spacing (m)	2.4	2.5	2.6	2.7	2.8	2.9	3	3.1	3.2
P (S > 1.5cm)	22.64	22.82	23.83	32.74	32.8	42.7	42.46	42.84	52.11
P (S > 2cm)	**0**	**0**	**0**	**1.72**	**1.9**	**6.75**	**6.93**	**6.94**	**12.26**
P (S > 2.5cm)	0	0	0	0	0	0	0	0	0
	Marl								
Anchor Spacing (m)	2.4	2.3	2.2	2.1	2	1.9	1.8	1.7	1.6
P (S > 1.5cm)	85.09	84.06	70.94	60.27	57.7	48.3	47.82	38.75	30.89
P (S > 2cm)	**34.8**	**34.78**	**27.31**	**21.61**	**20.3**	**15**	**14**	**9.65**	**4.83**
P (S > 2.5cm)	8.56	7.84	3.76	1.19	0.69	0.07	0.01	0	0
	Clay								
Anchor Spacing (m)	2.4	2.3	2.2	2.1	2	1.9	1.8	1.7	1.6
P (S > 1.5cm)	100	100	100	100	100	100	82.9	80	60.4
P (S > 2cm)	**95.45**	**72.21**	**54.46**	**52.67**	**37.3**	**23.7**	**8.89**	**7**	**0**
P (S > 2.5cm)	20.13	4.77	0	0	0	0	0	0	0

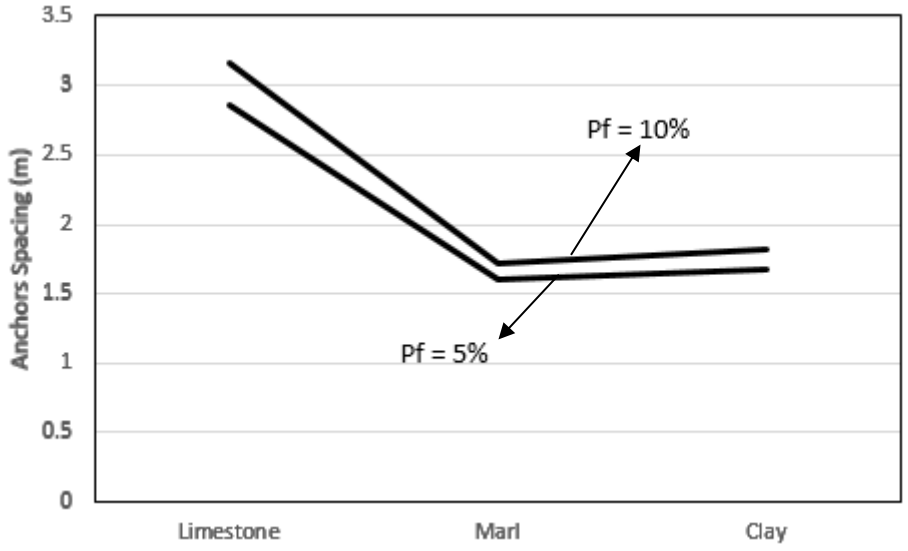

Figure 33. Anchors Spacing for Each Case at a Probability of failure of 5% and 10%

CHAPTER 6
CONCLUSION

6.1 Introduction

In this thesis, a database of 70 anchor pullout tests in geologic units involving limestone, marl, and clay was assembled and used to quantify the uncertainty in the bond stress – anchor slip relationship using a commonly used hyperbolic model. The statistics of the hyperbolic model parameters (a and b) can be used within a Monte Carlo Simulation framework to simulate bond stress – anchor slip curves that represent the expected variability in the anchor response in the bonded zone. Such curves are key to the serviceability limit state design of anchored retaining systems.

The hyperbolic model and the statistical parameters can be used to perform a reliability-based design on a design example where the deterministic design and the probabilistic design can be compared.

6.2 Summary of Findings

Based on the results of this study, the following findings, conclusions, and recommendations are made:

1. In order to check the serviceability-based design considerations for retaining walls that are supported with ground anchors a better understanding of the relationship of bond stress with anchor displacement in the bonded zone is needed. Also, more importance should be given to the uncertainties in the anchor design to increase the

safety and to optimize the design.

2. This study demonstrated that the observed uncertainty in the stress-displacement curves of anchor tests in Limestone, Marl, and Clay can be translated in the variability of two hyperbolic parameters. These hyperbolic parameters are used to normalize the stress-displacement curves using the linear regression method. Reliability-based design at serviceability limit state can be carried out using the obtained model.

3. Based on the results of the 70 tests in the three types of soil, it is indicated that the parameter "a" is more uncertain than the parameter "b" since the coefficient of variation for the "a" parameter is higher than the coefficient of variation for the "b" parameter. And these parameters shown the least variability in the case of Clay. Also, it is shown that the hyperbolic parameters are strongly negatively correlated.

4. After testing the CDFs of "a" and "b" against conventional lognormal probability distribution in addition to a more general four-parameter beta distribution that is limited in an interval [a b], it is shown that the beta distribution illustrate more realistically the uncertainty in "a" and "b" for all of the cases analysed. The statistical results of "a" and "b" are checked using 100 Monte Carlo simulations to make sure they reflect the real data.

5. A design example of an anchored retaining wall supporting two-layered soil is modeled on Wallap which is a software that does not take into consideration the displacement in the bonded zone. This design example can be used to make a

comparison between the deterministic and the probabilistic design. The case where the anchor is bonded in the clay layer showed the highest displacement while it showed the lowest displacement in the case of Limestone.

6. 10,000 Monte Carlo simulations of the two parameters “a” and “b” are generated in order calculate the probabilities of failure of the design example. The generated values are used to compute the displacement in the bonded zone which is added later to the displacement in the free zone to compute the total anchor displacement. The CDFs of the displacement in the bonded zone are tested against conventional lognormal and normal probability distributions in addition to beta distribution. For the three cases, the beta distribution illustrates more realistically the uncertainty in the displacement in the bonded zone

7. Using the probabilistic method allows the designer to consider the effect of uncertainties in the design. Relying on the probability of failure that was calculated using 10,000 generated values of “a” and “b” from Monte Carlo simulations, it seems that the design of the anchored wall in the case of limestone is too conservative. Which is not the case for the wall in the case of Marl and Clay where it is needed to decrease their probabilities of failure.

8. There is currently no link that is established between the resulting wall displacements at the location of the anchors and the mobilized pullout anchor force that was used in the design. Future work should focus on establishing this link through bond stress – anchor slip relationships that are similar to those established in this paper to couple the current ultimate limit state design methods with performance-based criteria that are related to the anchor displacement.

REFERENCES

Basha, B. M., and G.L.S. Babu. 2008. “Target reliability based design optimization of anchored cantilever sheet pile walls”. *Canadian Geotechnical Journal* 45 (4): 535-48.

Basma, A. A. 1991. “Safety and reliability of anchored bulkhead walls”. *Structural Safety*10 (4): 283-95.

Cherubini, C., A. Garrasi, and C. Petrolla. 1992. "The reliability of an anchored sheet-pile wall embedded in a cohesionless soil." *Canadian Geotechnical Journal* 29 (3): 426-435.

Ching, J., H. J. Liao, and C. W. Sue. 2008. "Calibration of reliability-based resistance factors for flush drilled soil anchors in Taipei basin." *Journal of Geotechnical and Geoenvironmental engineering* 134 (9): 1348-1363.

Dithinde, M., K. K. Phoon, M. De Wet, and J. V. Retief. 2010. "Characterization of model uncertainty in the static pile design formula." *Journal of Geotechnical and Geoenvironmental Engineering* 137 (1): 70-85.

Han, J, W. Zhao, and Y. Chen. 2017. "Design Analysis and Observed Performance of a Tieback Anchored Pile Wall in Sand." *Mathematical Problems in Engineering* 2017.

Hegazy, Y. A. 2003. "Reliability of Estimated Anchor Pullout Resistance." In *Grouting and Ground Treatment*, pp. 772-779.

Huffman, J. C., and A.W. Stuedlein. 2014. "Reliability-based serviceability limit state design of spread footings on aggregate pier reinforced clay." *Journal of Geotechnical and Geoenvironmental Engineering* 140 (10): 04014055.

Kim, N. K. 2003. "Performance of tension and compression anchors in weathered soil." *Journal of Geotechnical and Geoenvironmental Engineering* 129 (12): 1138-1150.

Kwon, M., J. Kim, H. Seo, and W. Jung. 2017. "Long-term performance of mechanically post-installed anchor systems." *Advances in Structural Engineering* 20 (3): 288-298.

Liu, X., J. Wang, J. Huang, and H. Jiang. 2017. "Full-scale pullout tests and analyses of ground anchors in rocks under ultimate load conditions." *Engineering Geology* 228: 1-10.

M. Zhang, J. Zhang, and L. L. Zhang, 185-202. Reston, VA: ASCE. Phoon, K. K., J. R. Chen, and F. H. Kulhawy. 2006. “Characterization of model uncertainties for augered cast-in-place (ACIP) piles under axial compression.” Foundation Analysis & Design: Innovative Methods (GSP 153), 82-89. Reston, VA: ASCE.

Najjar, S. S., E. Shammas, and M. Saad. 2014. “Updated normalized load-settlement model for full scale footings on granular soils.” Georisk: Asses. Manage. Risk Eng. Syst. Geohazards 8 (1): 3-80.

Najjar, S. S., E. Shammas, and M. Saad. 2017. “A reliability-based approach to the serviceability limit state design of spread footings on granular soil.” Geotechnical safety and reliability: Honoring Wilson H. Tang: Geotechnical Special Publication 286, edited by C. H. Juang, R. B. Gilbert, L.

Powers III, W. F., J. L. Briaud, and D. E. Weatherby. 1998. “Should grouted anchors have short tendon bond length?” *Journal of Geotechnical and Geoenvironmental Engineering* 124 (2): 110-119.

Prästings, A., S. Larsson, and R. Müller. 2016. "Multivariate approach in reliability-based design of a sheet pile wall." *Transportation Geotechnics* 7:1-12.

Zhao, W., J. Han and Y. Chen. 2018. "A numerical study on the influence of anchorage failure for a deep excavation retained by anchored pile walls." *Advances in Mechanical Engineering* 10 (2): 1687814018756775.